EFFECT OF SOIL STRENGTH AND VEGETATION ON MARSH EDGE EROSION FOR LOUISIANA COASTAL PROTECTION AND RESTORATION

Final Report

Undergraduate Research Opportunities Program (UROP)

Louisiana Sea Grant

Project Technical Area:	Living Resources: Recovery and Utilization	
Project Duration	Start Date: 03/01/2016	End Date: 12/31/2016

Student Name:	Brendan Copley
Major:	Civil Engineering
Department:	Civil and Environmental Engineering
Major:	Civil Engineering
E-Mail Address:	bcople1@lsu.edu

Faculty Advisor's Name:	PI: Navid H. Jafari	Co-PI: Qin J. Chen
Department:	Civil and Environmental Engineering	
Affiliation:	Louisiana State University	
Phone Number:	(225) 578-8475	
E-Mail Address:	njafari@lsu.edu	qchen@lsu.edu

ABSTRACT

Wetland loss along Louisiana's coast presents an urgent risk to natural habitats, coastal communities, and both local and national industries. A key natural cause of coastal erosion is continuous wave action along marsh edges. Moreover, coastal wetlands are frequently subject to surge and stronger wave forces brought about by tropical storms and hurricanes. The scarcity of synchronized field data of waves, currents, soil, and vegetation near a marsh edge limits the existing capability for predicting marsh edge erosion rate as a function of wave power, and soil and vegetation properties. The proposed research aims to enhance the fidelity of marsh edge erosion predictions for improved coastal restoration and management through data collection and the implementation of a continuously-monitored site in Terrebonne Bay. In-situ cone penetration tests will help determine the relationship between soil shear strength (across varying habitat types) on erosional resistance. Spatial and temporal trends in soil strength are anticipated to clarify why certain locations erode faster than other areas. The proposed methodology for marsh edge monitoring incorporates photogrammetry through the placement of cameras at frontal and lateral views. This novel approach will be used to identify the frequency and evolution of marsh retreat, and will assist long-term efforts at developing a mechanistic erosion model. The success of future marsh creation projects implemented by state agencies will be fortified by a more robust understanding of the geotechnical parameters affecting marsh edge erosion and the physical processes that lead to coastal land loss.

1. INTRODUCTION

Wetland loss on the hurricane-prone Louisiana coast continues at notably high rate. During the period of 1932-2010, the total land loss in coastal Louisiana was 1,833 mi^2, and the rate of loss from 1985-2010 was 16.6 mi^2/yr (Couvillion et al. 2011). This figure is often presented to the public in rather alarming terms: Louisiana is losing a football field of wetlands every hour. The reasons for wetland loss are complex and both natural and anthropogenic in origin. These include subsidence from sediment compaction and dewatering, eustatic sea-level rise, growth faults, isostatic adjustments, and erosion due to waves and storm surges. Regional anthropogenic causes include channelization of the Mississippi River, canal dredging through wetlands, and fluid withdrawal (e.g., groundwater, hydrocarbons). One of the important natural causes of coastal erosion is the constant wave action on the marsh edges. Analysis by Penland et al. (2000) shows that 26% of the wetland loss in the Mississippi River Delta from 1932 to 1990 can be attributed to erosion due to wind waves. Additionally, coastal wetlands in this region also experience frequent surge and stronger wave forces resulting from tropical storms and hurricanes. To combat the devastating wetland loss, the latest draft of Louisiana's Comprehensive Master Plan for a Sustainable Coast (CPRA 2017) has prioritized sediment diversions, shoreline protection, and marsh creation projects. In fact, marsh creation projects constitute the nation's largest investment, totaling over $20 billion, in the 2017 Draft Coastal Master Plan (CPRA 2017).

Seven predictive models were utilized to develop and assess the efficacy of the 2012 Coastal Master Plan (CPRA 2012). Among them is the Wetland Morphology Model, which forecasts the wetland changes with and without coastal protection and restoration projects in the next 50 years (Allison et al. 2015). One of the suggested improvements for the wetland morphology model is to explicitly consider marsh edge erosion and vegetation-dependent accretion in the forecast of wetland morphological changes. The rate of erosion at the marsh edge is a key parameter for predicting the longevity of a given vegetated marsh, including future marsh creation projects. The soil and plant types, along with hydrodynamic characteristics, are the controlling variables for the rate-of-retreat at marsh edges. However, there is a lack of synchronized field data of waves, currents, soil, and vegetation near a marsh edge. Consequently, the existing capability of predicting the marsh edge erosion rate as a function of wave power, and soil and vegetation properties is rather limited. Our research group is focused on developing a robust marsh edge erosion model that incorporates hydrodynamic, soil, and vegetation properties

and is calibrated to coastal Louisiana. A more robust wetland morphology model that includes marsh edge erosion will improve our ability to forecast the impact of coastal protection and restoration projects and assist in managing of Louisiana's coastal resources.

The proposed project aims to enhance the fidelity of marsh edge erosion predictions in coastal Louisiana, specifically in Terrebonne Bay and Breton Sound, for improved coastal restoration and management. The major objectives are: (1) to identify the soil and vegetation properties that influence erosional resistance; and (2) to propose a field-validated marsh edge erosion model that incorporates coastal, geotechnical, and ecological engineering parameters. The project's primary objectives are to identify the soil and vegetation properties that influence marsh edge resistance to erosion; and produce a field-validated marsh edge erosion model for the Terrebonne Bay and Breton Sound areas that incorporates coastal, geotechnical and ecological engineering parameters. Research has elucidated some of the key mechanisms controlling marsh edge erosion, including wind-generated waves (Chen et al. 2005; Priestas et al. 2015), presence of vegetation (D'Alpaos et al. 2007), erosion of cohesive sediment (Black et al. 2002), anthropogenic factors (Gedan et al. 2009), and soil properties (Feagin et al. 2009; Howes et al. 2010). The experimental work by Feagin et al. (2009) suggests that soil type is the primary variable that influences wave-induced erosion. Howes et al. (2010) used the shear strength of soil to explain the failure of low- and high-salinity wetlands during Hurricane Katrina. Both studies conclude that the type and properties of marsh soils are important factors to consider when comparing erosion rates among sites, yet existing prediction models for marsh stability and evolution (e.g., Schwimmer (2001) and Mariotti and Fagherazzi (2010)) predominantly focus on wave power and lump soil and vegetation effects into field-calibrated empirical constants.

Attempts to predict marsh edge retreat rate using only wave power have met varying levels of success. Schwimmer (2001) first quantified marsh boundary retreat rates in a study of various sites along Delaware's Rehoboth Bay. Retreat rates obtained by local shoreline surveys over a five-year period were used to compute the average land loss over a given shoreline length. Wind, bathymetric, and fetch data were used to hindcast the wave climate from which the total averaged wave power at each site was computed. Based on this approach, Schwimmer (2001) proposed $R = 0.35P^{1.1}$, where R is erosion rate (m/yr), P is wave power (kW/m), and 0.35 and 1.1 are field-calibrated empirical constants that account for soil type, water elevation, vegetation, and macrofauna. Similar to Schwimmer (2001), Parker (2014) analyzed aerial imagery from 1998 to

2010 to estimate the historical retreat rate of shorelines found in Terrebonne Bay. He supplemented the historical retreat rates with GPS shoreline surveys conducted over a period of 12 months and deployed wave gauges to determine the wave characteristics directly in front of the marsh edge. The recorded wave gauge data was used in Delft3D to obtain water levels in the bay, which was then input into a SWAN model to estimate the average wave power. As a result, Parker (2014) developed Fig. 1 to relate the average wave power and retreat rates at 28 sites within Terrebonne Bay. Although retreat rates generally increase as the wave power increases (R^2 = 0.17), Fig. 1 indicates that the predictive power of erosion rate using only wave power is limited. Therefore, the inclusion of spatially varying, site-specific soil strength and vegetation in addition to the hydrodynamic driving force is a logical step towards improving a predictive model for marsh edge erosion. This project will demonstrate marsh edge erosion is a function of soil, vegetation, and wave characteristics. We hypothesize that a strong trend exists between wave energy and local site-specific erosion, but expanding from localized areas to a regional scale the magnitude of erosion likely depends on other ecological and geotechnical parameters.

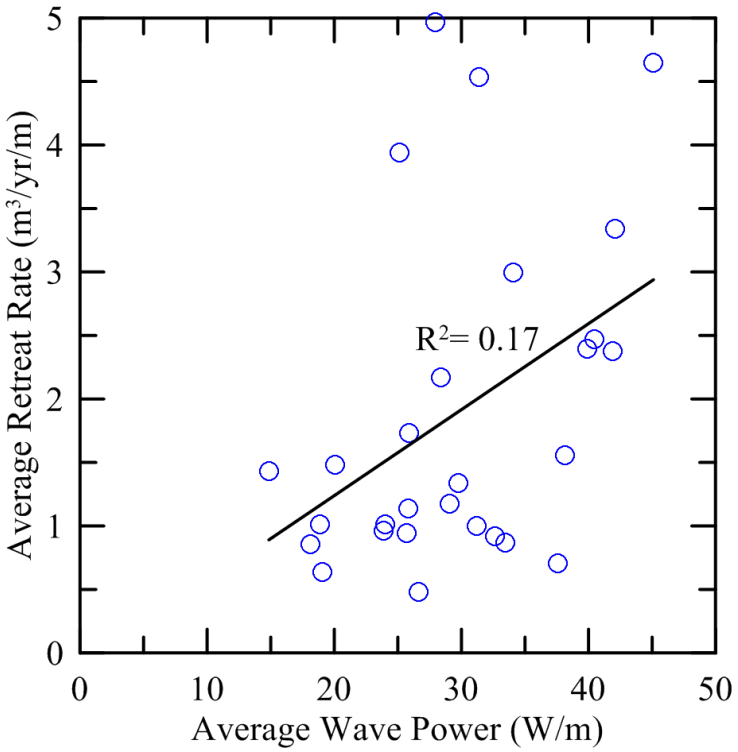

Fig. 1. Marsh edge erosion rate derived from GIS shoreline analysis and average wave power computed from SWAN and Delft3D models for 28 sites across Terrebonne Bay, LA (data from Parker 2014)

2. LITERATURE REVIEW

Existing literature on marsh erosion consists of laboratory, model, and field studies. The laboratory literature reviewed primarily focuses on understanding the failure model (viz., undercutting, toppling, and surface erosion) using field or reconstituted samples. Model studies are divided between hydrodynamic and erosion considerations, which are further subdivided into parametric/analytical, numerical, empirical, and theoretical approaches. Field investigations represent a significant portion of marsh erosion studies. Investigators obtained a variety of measurements, focusing on vegetation and soil properties, retreat rates, and/or wave characteristics. Models for predicting marsh erosion retreat rate and/or failure mode are divided into empirical and theoretical models, wherein the theoretical models include field derived, laboratory derived, and limit equilibrium methods. The empirical models are typically used for predicting marsh erosion for coastlines, whereas the theoretical models are focused on failure models and individual events or for understanding the long-term evolution of salt marshes and tidal flats. More recently, semi-empirical models for coast-wide erosion predictions include wave and geotechnical properties.

Geotechnical measurements for marsh erosion studies have focused on shear strength, physical index properties, and erodibility. Soil shear strength has been predominantly measured using some form of vane shear apparatus (e.g., field vane, lab vane, torvane, wetland soil strength tester). The differences lie in the size, number, and shape of the blades used as well as the sample volume tested. In each case, values are obtained by measuring the torque required to rotate the vane, which is later converted into a soil shear strength. Laboratory measurements include unconfined compression tests, but these are performed much less frequently because of the difficulty in sampling marsh soils due to soil disturbance and compaction in the sample tube. However, sampled soils are often taken to the laboratory for testing on physical properties, including bulk density, organic matter content, grain size, and soil classification. While the erosional resistance of soils has been measured in both field and laboratory settings, these studies mainly focus on cohesive sediments in the mudflat rather than the marsh surface.

2.1 Geotechnical Testing

Studies have stressed the importance of shear strength for marsh erosion by indicating the observed failure mechanisms are dominated by shearing of mass blocks (Knutson 1987; Pestrong

1972; Redfield 1972). Geotechnical investigations involving in-situ tests to measure shear strength have been formalized via American Society for Testing and Materials (ASTM) standard test methods (e.g., ASTM D2573 (2015) and ASTM D5778 (2012)). However, there are no ASTM methods for determining the shear strength of coastal wetland soils, which are typically very soft, cohesive sediments with high organic matter contents and oftentimes extensive root mats, and which are flooded or at least saturated with water during high tide. Multiple instruments have been used to measure the shear strength of marshes, including the field inspection vane (Chen et al. 2013; Howes et al. 2010; Turner 2010), wetland soil strength tester (Sasser et al. 2013), torvane (Wilson et al. 2012), and mechanical cone penetrometer (Are et al. 2002). The mechanical cone penetrometer provides measures of tip resistance and sleeve resistance continuously with depth (Robertson 2009), while the field vane apparatus measures the undrained shear strength at discrete intervals. The vane apparatus was designed for soft, homogenous clay deposits and the results are typically used for designing earthworks and foundations. The blade width for the field vane, miniature vane, and torvane are 2.55 in. (65 mm), 0.63 in. (16 mm), and 0.75 in. (19 mm), respectively. The wetland soil strength tester (WSST) was designed only as a surface test for quantifying root mat strength (Sasser et al. 2013). Examples of each instrument are provided in Fig. 2.

Turner (2010) used the field inspection vane to test soil sustainability and increased nutrient loading to marshes. He reports the shear strength profile is at its greatest near the surface and decreases to a range of 3-6 kPa at depths below 20 cm. Shear strengths begin to increase linearly after a depth of 80 cm. This general observation was also verified by Are et al. (2002) and (Day et al. 2011) using mechanical cone penetrometers. Howes et al. (2010) measured shear strength of high- and low-salinity soils using the vane and found a statistical difference in shear strength. Wilson et al. (2012) also found a correlation of higher shear strength at marsh platforms compared to readings from dieback, creek head, and re-vegetated areas. Sasser et al. (2013) designed the WSST to determine if marsh soil shear strength measurements are associated with plant biomass variables and if soil strength varies among different vegetation types. They sampled 52 sites within Louisiana's CRMS-*Wetlands* program (CPRA 2017), comprising 11 marsh types and a total of 227 WSST measurements. They report living belowground biomass was the most consistent indicator of marsh soil strength. In coastal marshes that contain roots and shell fragments, the vane shear strength will be artificially increased and inconsistent. This constitutes a significant

drawback of the vane shear device. A direct comparison of these instruments is also difficult because they measure the response of different physical soil behavior, through measuring soil strength by displacing soil at different depths, or by way of integrating over different areas or in different directions (i.e., horizontal vs. vertical). In addition, soil strength in coastal marsh environments is typically expected to be more variable than in other environments due to an abundance of biomass, pore water, organics, and widely varying grain-size distributions. The results of this review indicate that there is a need to identify and develop an in-situ methodology to assess marsh shear strength over a full range of vegetation types and environmental conditions.

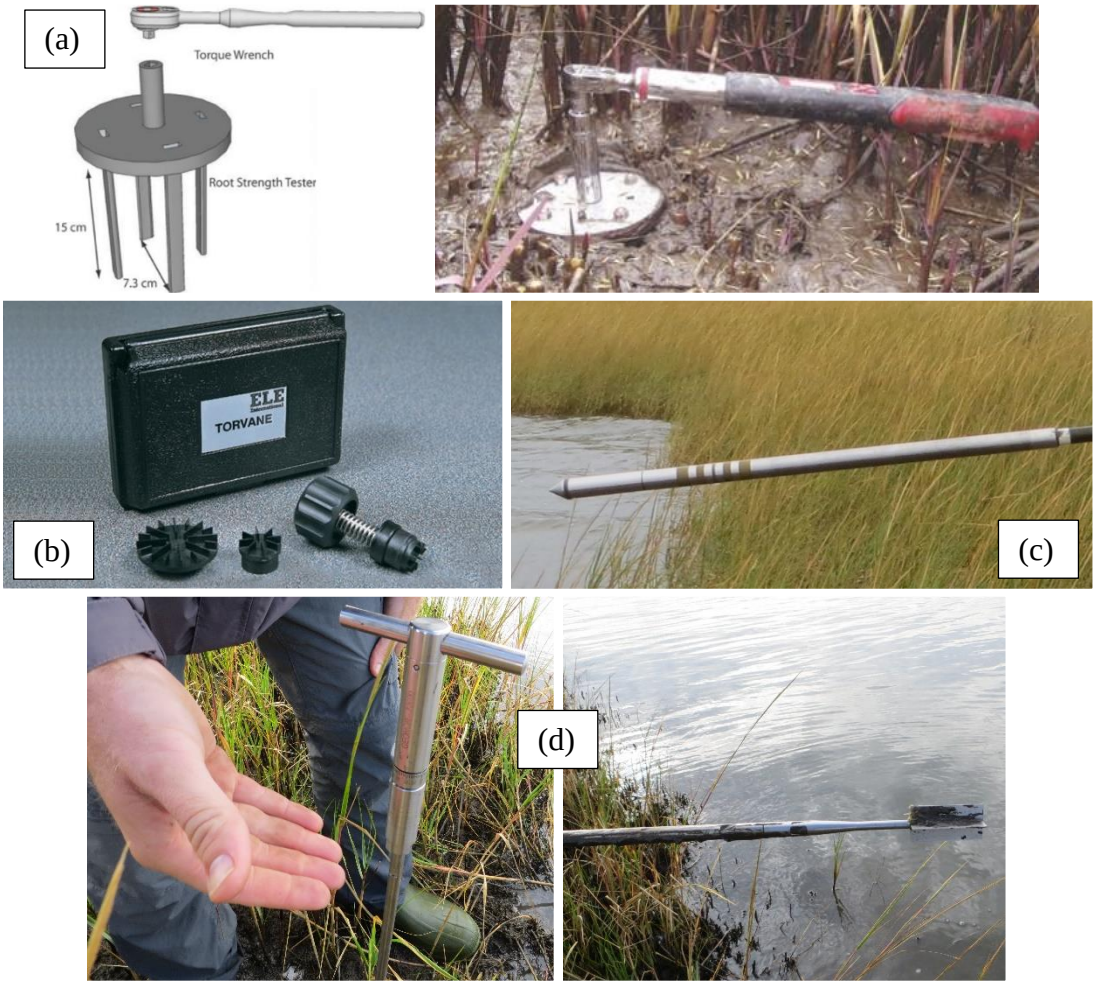

Fig. 2. Examples of instruments used to measure shear strength of marshes: (a) WSST (image adapted from Sasser et al. 2013), (b) torvane shear device (image courtesy of ELE International, Leighton Buzzard, England), (c) electric piezocone penetrometer (image by Navid H. Jafari), and (d) Geonor H-60 hand-held vane tester (image by Qin J. Chen)

This lack of a uniform assessment methodology creates uncertainty when comparing different investigations on marsh soils and adds complexity for attempting to draw broad conclusions from multiple sites across Louisiana, other U.S. states, and the world.

In addition to shear strength, studies have measured the physical properties of wetlands. These include bulk density, organic matter content, pH, grain size distribution, and redox potential. These parameters are typically used to classify the soils (e.g., clays, silts, and organics). Bulk density and organic matter content are strong indicators of stratigraphy because they can differentiate between highly organic soils and mineral sediments. However, these properties do not correlate to shear strength and, except for bulk density, are not incorporated in marsh erosion/stability models. In the same context, erosional resistance has been measured using a cohesive strength meter (Chen et al. 2013), benthic flume (Amos et al. 1992), gust chamber (Lo et al. 2014), and erosion function apparatus (Briaud et al. 2006). However, most of these studies focus on the erodibility of cohesive sediments and their application to marsh erosion may be limited because the predominant failure mode reported therein is mass block failure.

2.2 Erosion Models

The marsh erosion models were divided into semi-empirical and theoretical methods, where the semi-empirical models applied to coast-wide marsh retreat predictions and theoretical models focused on individual failure events. Through this literature review, the theoretical models are further classified into limit equilibrium, laboratory derived, and field derived methods. Still, most marsh erosion models are semi-empirical, which likely results from of a lack of understanding of the progression of failure and mechanics and uncertainty in input parameters (e.g., shear strength, vegetation, hydrodynamic forcings).

The limit equilibrium method is the commonly used technique of evaluating instabilities for landslides, man-made slopes (e.g., levees, highway embankments, landfills), and riverbanks. In particular, the Bank Stability and Toe Erosion Model (BSTEM) is an approximate analogy to marsh edge erosion because, as the name suggests, it includes both stability and toe erosion. Developed at the USDA-ARS National Sedimentation Laboratory, BSTEM and its functions are discussed at length by Pollen-Whitehead and Simon (2009; 2010). The stability model can compute the factor of safety using a number of methods: horizontal layers per Simon et al. (2000), vertical slices with a tension crack per Morgenstern and Price (1965), and cantilever failures per

Thorne and Tovey (1981). The model accounts for soil strength of multiple layers, partially-variable saturated soils (i.e., positive and negative pore-water pressures), confining pressure due to streamflow, and soil reinforcement and surcharge due to vegetation. The toe erosion model is used to estimate the bank and toe erosion, which is subsequently incorporated into the stability model. The erosion is predicated on hydraulic shear stress, as determined by channel geometry, and the soil's critical shear stress and erodibility parameters. While BSTEM incorporates key parameters into its stability analysis that relate to marsh edge erosion (e.g., soil and vegetation strengths, pore-water pressures, toe erosion), there are several distinct differences between the two environments. For example, toe erosion in BSTEM is estimated from shear stress parallel to the bank, while waves breaking along a marsh edge impose perpendicular shear stresses. In addition, the dynamic impact force on the marsh bank from waves can contribute to instability through additional sediment erosion and increased pore-water pressure within the bank's constituent soil. The model assumes hydrostatic conditions and therefore does not explicitly model transient seepage. This is important to note because still water levels near marshes can vary substantially over short periods due to tides and cold fronts, whereas river levels (at a given cross-section) are relatively constant over time.

Laboratory- or field-derived models have been primarily developed for a given failure mode observed in the wave flume experiment or field. Bendoni et al. (2014) use a wave flume to replicate the toppling mass failure due to oscillating waves. They instrumented vegetated and unvegetated banks with pressure transducers, micro-tensiometers, and water content sensors to understand the dynamic soil response to waves. The governing equation for predicting failure comes by solving for the rotation of a block, which is assumed to be a rigid and impermeable body that follows viscoelastic behavior per the Kelvin-Voigt model. The failure plane is horizontal, and the failure criterion is equated to the tensile strength of the material (Fig. 3a). Hydrostatic and dynamic forcings are incorporated by estimating wave thrust and soil damping. Bendoni et al. (2014) found the conditions of (1) water inside the tension crack and (2) low water levels in front of the bank are the most unfavorable for promoting bank instability. This study indicates that the dynamic response of the system appears to be crucial in predicting bank instability, as several factors, such as elastic potential energy accumulated by the system during compression and released during the wave draw-down, and inertial effects, lead to higher stresses.

The field-derived model by Gabet (1998) replicates the undercutting failure mechanism for

California estuaries. In this case, undercutting creates a cantilever soil block (Fig. 3b). This simple static model determines the moment at the end of the cantilever, where the failure criterion is determined from the driving moment of the weight of the block and soil-vegetation shear strength. The model is used to estimate the width of undercutting before a failure occurs, which signifies lateral retreat of the marsh. Another field-derived model was proposed by Bendoni et al. (2016). In Fig. 3c, Bendoni et al. (2016) separate erosion into two layers based on the still water level and wave characteristics. In this case, soil erodibility and undercutting are incorporated into the model. If the toe face retreats at a faster rate than the top face, undercutting will form and eventually leads to a mass failure when a threshold length is exceeded. This model also accounts for the still water level. For example, the top face only erodes when the still water level is at or above the height of the toe face. In other words, the toe face will not erode if submerged and the top face will not erode if the still water level is not acting on the vertical length. The length of erosion for top and toe faces is a function of an assumed soil erodibility and wave power.

Semi-empirical models estimate marsh erosion by correlating observed retreat rates (based on aerial imagery, erosion pins, terrestrial GPS surveys, etc.) with predicted and/or measured wave characteristics. Schwimmer (2001) quantified marsh boundary retreat rates over a five-year period along sites within Rehoboth Bay, Delaware. Retreat rates obtained by local shoreline surveys were used to compute the average land loss over a given shoreline length. Wind, bathymetric, and fetch data were used to hindcast the wave climate from which the total averaged wave power at each site was computed. Based on this approach, Schwimmer (2001) proposed Eq. (H) using an empirical time-averaged erosion rate (R, m/year) as a function of wave power (P, kW/m). Marani et al. (2011) derived a linear relationship between volumetric retreat rate (V, m^2/yr) and mean wave power density (P, kg-m/yr^3) using Buckingham's theorem of dimensional analysis. The authors calibrated the average volumetric erosion rate (Eq. I) by determining the erosion rates along 150 sites inside the Venice Lagoon, Italy, using historical aerial imagery and utilizing a parametric wind model to estimate wave power. Priestas et al. (2015) used marsh retreat rates obtained from pins and shoreline surveys at 33 sites in Hog Island Bay, Virginia, to develop Eq. (J) in terms of wave power. Leonardi and Fagherazzi (2015) added an exponential function to Eq. (H) to account for variability in soil resistance (H_c) and mean wave height (H). They calibrate Eq. (K) with three sites along Plum Island Sound, Massachusetts, using the cell automata model. Mariotti and Fagherazzi (2010) developed an eco-geomorphic model to study the long-term evolution of salt

marshes. To replicate marsh erosion, they emulated the formula for mud erosion, $R = \alpha(\tau - \tau_c)$, by including a critical wave power threshold (P_{cr}) and empirical constant (β) calibrated to produce retreat rates in practical units (i.e., m/yr). Because this study investigated hypothetical cases, the model (Eq. L) was not validated against field or laboratory data.

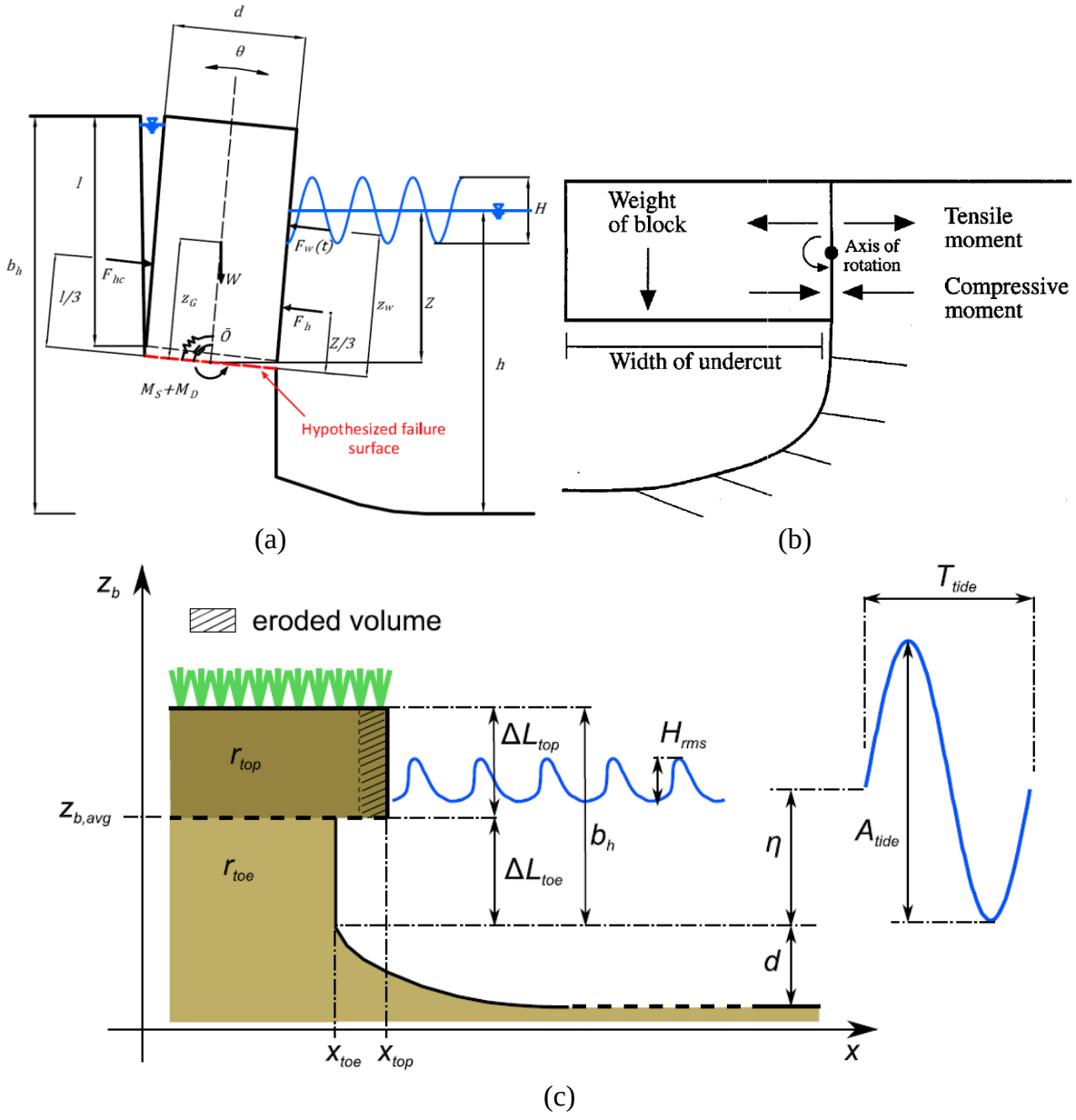

Fig. 3. Examples of theoretical models: (a) Bendoni et al.'s (2014) toppling mass failure showing forces acting on a rigid block, (b) Gabet's (1998) undercutting formulation using moment of cantilever, (c) Bendoni et al.'s (2016) field-based erodibility of two layers and undercutting-of-mass failures

Table 3. Summary of semi-empirical marsh erosion models

Study	Model Equation		Parameters
Schwimmer (2001)[a]	$R = 0.35P^{1.1}$	(H)	▪ R (m/yr): local shoreline surveys ▪ P (kW/yr): average wave power, hindcast from historical wind, bathymetric, and fetch data
Marani et al. (2011)[b]	$V = 0.03P + 0.19$	(I)	▪ V (m^2/yr): historical imagery, assumed scarp height ▪ P (kg-m/yr^3): parametric wind model
Priestas et al. (2015)[c]	$R = 0.079P + 0.43$	(J)	▪ R (m/yr): pin and shoreline surveys ▪ P (kW/m): SWAN
Leonardi and Fagherazzi (2015)[d]	$R = 0.35P^{1.1} \exp\left(-\frac{H_c}{H}\right)$	(K)	▪ R (m/yr): GPS surveys ▪ P (kW/m): per Young and Verhagen (1996) ▪ H_c (m): equal to $4 \cdot S_u/\gamma$ ▪ S_u (kPa): measured by vane shear apparatus ▪ γ (kN/m^3): saturated unit weight ▪ H (m): mean wave height
Mariotti and Fagherazzi (2010)[e]	$R = \beta\left(P - P_{cr}\right)$	(L)	▪ β: empirical factor ▪ P: per linear wave theory ▪ P_{cr}: critical wave power, a function of biomass

[a] Based on surveys of Rehoboth Bay, DE
[b] Based on surveys of Venice Lagoon, Italy
[c] Based on surveys of Hog Island Bay, VA
[d] Based on surveys of Plum Island Sound, MA
[e] Based on a hypothetical location

Recent attempts to develop theoretical and empirical marsh-edge retreat rate models have met varying levels of success. This may be due to several reasons, including a lack of knowledge of the mobilized failure mode and corresponding mechanistic formulations, missing input parameters (e.g., geotechnical, ecological, marsh profile), and temporal incompatibility. The theoretical models discussed herein (Bendoni et al. 2014; Bendoni et al. 2016; Gabet 1998) capture two failure modes (undercutting and soil erodibility) at varying degrees of complexity. These models highlight the need to account for the failure mode, as undercutting failure is found to control the retreat rate. The simplistic nature of each model stems from insufficient observations of the progression of failure in the field. The long-term goal of the theoretical models is to achieve a level of sophistication similar to that of BSTEM and geotechnical slope stability models based on limit equilibrium or finite element methods. Johnson (2016) represent the first models to incorporate shear strength in their formulations. The marsh profile can also play an influential role; for example, the marsh platform and mudflat elevations control the wave power estimates. Thus, an area of future research is developing models that include geotechnics (shear strength, wave damping), ecology (vegetation type, roots), and marsh profile in the semi-empirical models.

Bendoni et al. (2016) compared short-term (weeks to months) to long-term (years to decades) retreat rates reported by Marani et al. (2011) and found the short-term rates to be much greater. They explained this observation using the analogy to the dependence of the rate of bed load transport on sampling frequency described by Singh et al. (2009). Longer time scale observations tend to smooth out higher peak fluctuations and include both variations intrinsic to the physical processes at work and possible changes in external forcing (e.g., variation due to human activities or climate change). As a result, these findings suggest there is an important need to develop process-based, mechanistic models for investigating possible long-term evolution of marshes by carrying out field observations on short time scales.

3. SITE INVESTIGATION

Fig. 4 shows an overview of Terrebonne Bay, Louisiana, and the three sites investigated to obtain geotechnical and morphological characteristics. Site 1 has historically experienced low erosion rates, whereas Sites 2 and 3 have experienced high erosion rates. There were multiple locations within each site where the CPTu parameters, scarp height, marsh elevation, and morphologic profile were measured. In total, 25 locations were visited during the field work.

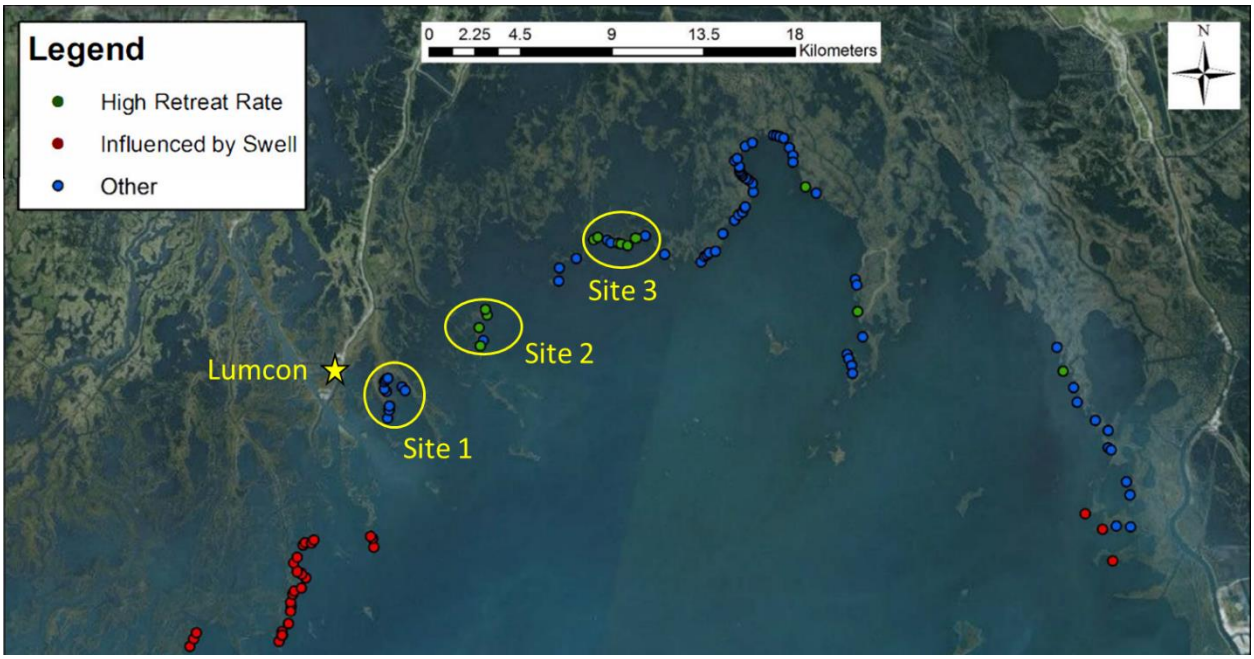

Fig. 4. Overview of visited sites in Terrebonne Bay (image courtesy of Thomas O. Everett)

3.1 Cone Penetrometer

The piezocone penetrometer provides a continuous profile of soil shear strength and other geotechnical parameters, namely pore pressure, shear wave velocity, moisture content, and electrical resistivity (Robertson 2009). However, the weight of the push frame and drive system of the penetrometer make it prohibitive for carrying in wetlands, thus applications in coastal marshes have been limited. To overcome these restrictions, Dr. Jafari's research group has developed a lightweight push frame that is hand-operated and easier to maneuver through the wetlands than a typical hydraulic rig mounted on a truck or marsh buggy. The push frame consists of an aluminum frame inserted into the ground to provide stability and verticality during penetration. In addition, the LSU piezocone penetrometer is superior to a typical cone penetrometer because it captures environmental parameters (soil moisture, resistivity, and temperature, collectively abbreviated as SMRT) in addition to geotechnical parameters (tip resistance, sleeve friction, and pore pressure). Fig. 2c shows an enlarged image of the CPTu apparatus with the attached SMRT module and locations of each sensor. The soil resistivity is directly measured across a resistor, while the measured soil dielectric constant is correlated to volumetric moisture content using Topp et al. (1980). To perform a cone sounding, the cone is inserted through the frame and connected to the depth recorder and laptop. As the cone is hand-pushed into the marsh at a rate of approximately 2 cm/s, the laptop reads the output at 2-cm increments (i.e., a total of 125 readings are collected for a 2.5-m sounding). The tip resistance (q_c) and pore-water pressure (u_2) readings are used to determine the corrected tip resistance, $q_t = q_c + u_2 (1–a)$, where a is the cone's unequal area ratio (equal to 0.8). The undrained shear strength is determined as $s_u = (q_t – \sigma_v)/N_{kt}$, where the empirical factor N_{kt} is assumed to be 20 for soft and clayey Louisiana soils (CPRA 2015). The SMRT-CPTu device was used to determine the soil shear strength at the three general sites in Fig. 4. The environmental parameters (soil resistivity and volumetric moisture content) will be correlated to in-situ salinity, bulk density, and belowground biomass to develop geotechnical-ecological relationships for saline marshes and corresponding plant species (e.g., *Spartina alterniflora*).

Fig. 5 shows the step-by-step procedure to perform a CPTu sounding. The depth recorder is attached to the cone stand, which is subsequently anchored into the ground for stability. The cone is placed through the center slot and a string is attached from the depth recorder to the cone push rods. The cone is pushed at a consistent rate for the full depth range of 2.5 m.

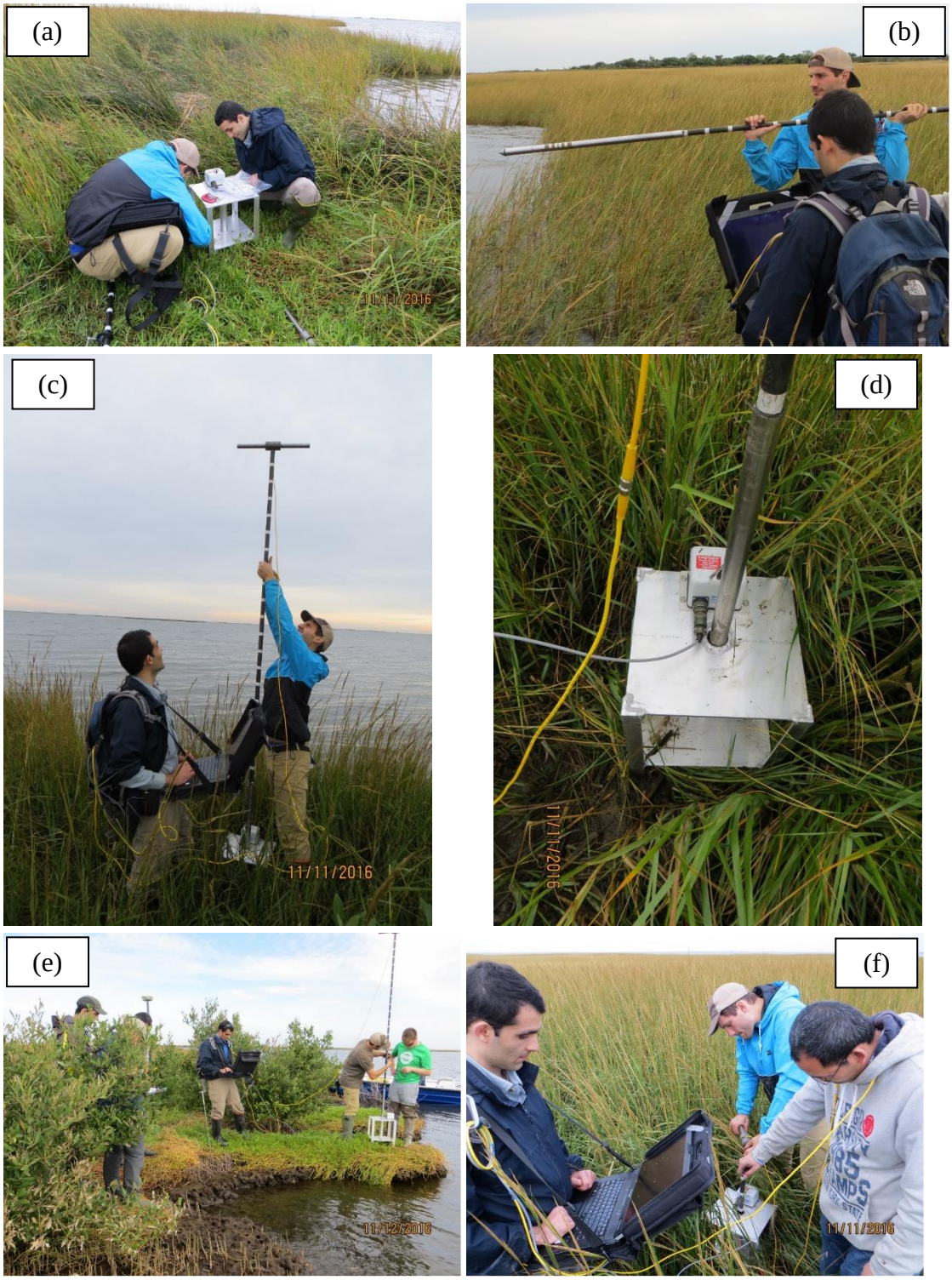

Fig. 5. CPTu testing procedure: (a) placement of testing platform with depth recorder attached, (b) baseline readings recorded via data acquisition software, (c) cone penetrometer guided through the testing platform, (d) cone penetrometer in position prior to soil insertion, (e) depth recorder string attached to the rod extension approximately 1 m above the testing platform, and (f) cone penetrometer fully inserted at the end of testing

3.2 Marsh Elevation and Profile

To measure the marsh elevations and profiles, a Trimble R8 GNSS (Global Navigation Satellite System) field unit capable of Real-Time Kinematic surveying (RTK) was obtained from the LSU Center for GeoInformatics (C4G). The marsh surface elevation was surveyed to an accuracy of 1 cm. The Trimble unit was also used to map the location of each CPTu and field vane test so that a spatial map of the tests would be available for future field campaigns. Figs. 6 and 7 show the Trimble RTK unit components, including the GNSS antenna, GSM radio, and hand-held controller, all mounted on a standard 2-m carbon fiber rod.

Fig. 6. Measuring scarp height using a metric ruler (left) and RTK unit (right)

Fig. 7. Configuring the RTK unit to record location of a recently completed cone penetration test

3.3 Time-Lapse Camera

Although laboratory and field observations suggest three marsh edge erosion mechanisms are prevalent (slumping, undercutting, and root scalping), long-term continuous monitoring has not been performed to understand the time-dependent erosion process. As a result, we recently installed a Brinno TLC200Pro camera (encased in weather-resistant housing) to identify the progression of marsh erosion using time-lapse imaging. The camera was mounted on an open-ended steel pipe that was driven sufficiently into the ground to provide an adequate foundation capable of resisting wave and wind forces (Fig. 8). The camera is angled at an oblique view to the shoreline to monitor the waves impacting the marsh edge. The photos will be collected on a subsequent field trip and analyzed for developing a framework for the progression of marsh edge erosion.

Fig. 8. Time-lapse camera after installation

4. PRELIMINARY CPTu RESULTS

Three to four CPTu soundings were conducted in close proximity to each other at each location within Sites 1 to 3. Approximately 75 CPTu soundings were performed, in total. Soundings from each testing location were compiled together to develop an understanding of the spatial variability of the soil and identify any aberrations in the collected data. Five parameters were plotted with depth: tip resistance (q_c), sleeve friction (f_s), pore-water pressure (u_2), volumetric moisture content (w), and soil resistivity. Fig. 9 shows two typical subsurface profiles observed in Terrebonne Bay, in which Fig. 9a and Fig. 9b show sites with high and low erosion rates, respectively. For example, the q_c trend in Fig. 9a shows slightly higher resistance at the surface

due to penetration of vegetation before the values decrease to a minimum strength from 0.15 to 1.25 m. The tip resistance begins to gradually increase after a depth of 1.25 m, indicating a stronger foundation layer consisting of deltaic sediments is present. The sleeve friction results corroborate this behavior because some adhesion was measured on the sleeve at shallow depths (vegetation effect) before it reduced to zero until a depth of 1.25 m, where it increased with depth like the q_c plot.

The volumetric moisture content profile matches the q_c and f_s plots. The high volumetric moisture contents of ~80% likely represent the vegetative mat and saturated organic-rich layer. A clear delineation between the vegetative mat to organic layer was not found but it postulated that the vegetative mat is the zone from 0 to 0.15 m where the volumetric water content varies more. The interface from organic-rich layer to the foundation layer was evident from the decreasing volumetric moisture content with depth. This trend suggests the soils consist of mostly inorganic sediments with small concentrations of organics. Fig. 9a also reports the pore-water pressure (u_2) which generally increased with depth, and the soil resistivity, which was approximately constant with depth. In contrast to Fig. 9a, Fig. 9b shows that a stronger foundation layer is not present for this test location. In particular, tip resistance remains at or below 50 kPa (similar to the q_c range in Fig. 9a) for the entire depth of penetration. This trend was also supported by the volumetric moisture content because values remain above 85% and do not show any evidence of decreasing. The vegetative mat in Fig. 9b was assumed to be slightly thicker than Fig. 9a because of the variability in values after 0.4 m decreased and the lines plotted on top of each other. In summary, the preliminary results from the CPTu soundings demonstrate this method's capacity for identifying the soil stratigraphy of salt marshes and corroborate the presumption that lower shear strengths correlate to higher erosion rates. However, the data analysis of the cone tests is still ongoing. Results from all 22 locations from Sites 1 to 3 are presented in the Appendix.

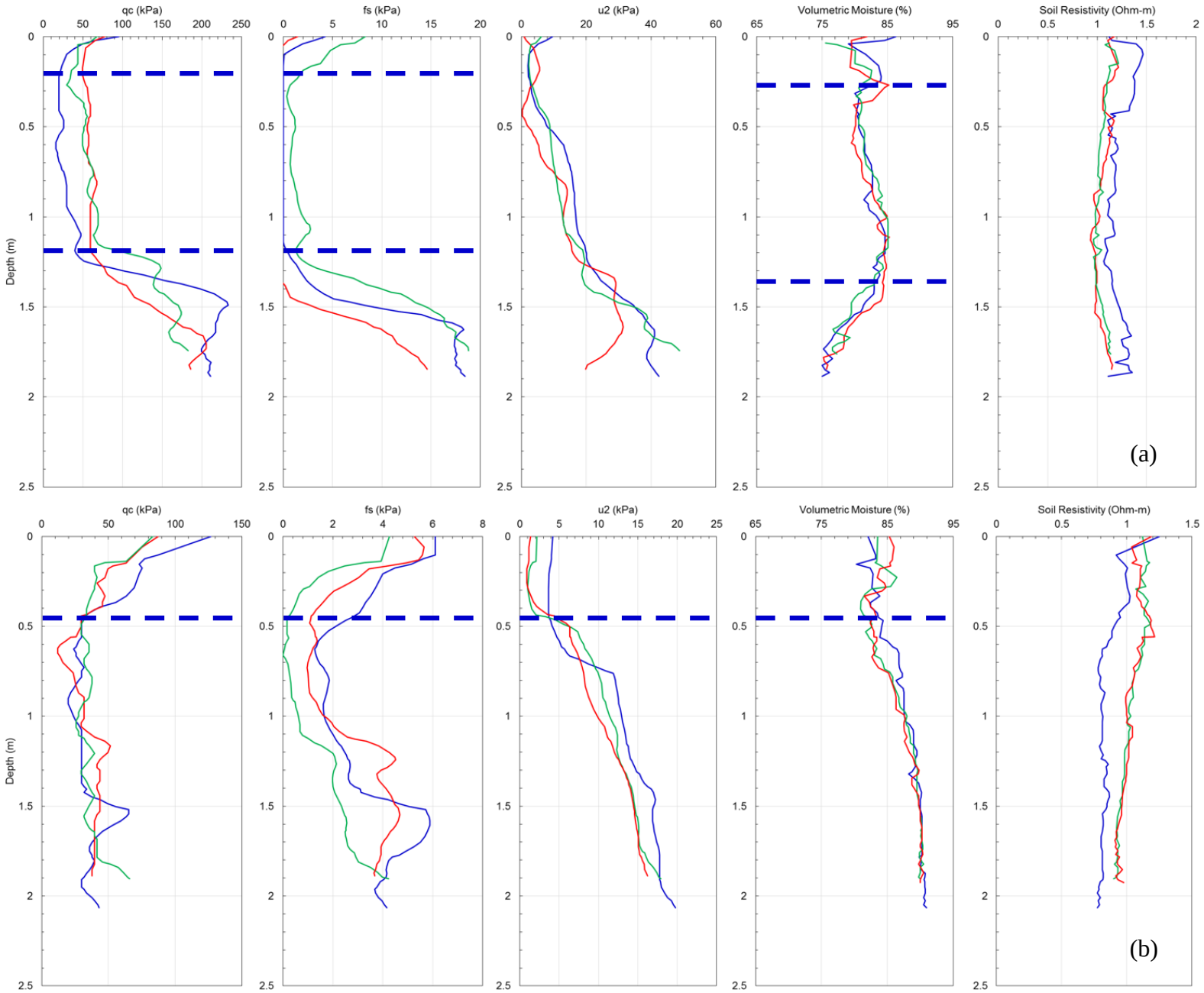

Fig. 9. Preliminary CPTu results for (a) low erosion-rate site with foundation layer present and (b) high erosion-rate site with no foundation layer present

5. PRELIMINARY MARSH PROFILES

The rationale for obtaining the marsh profiles was to characterize the underlying mechanism of marsh edge erosion (e.g., undercutting, root scalping, and/or block or toppling failure). Fig. 10 presents examples of the morphology of marsh edge for sites that experienced both high and low erosion rates. In general, two profiles were observed. The first is a steep scarp followed by a gently-sloping tidal flat. The second profile is more representative of a concave-upward shape, similar to the equilibrium profile formulated by Wilson and Allison (2008). The dominant failure mechanism observed at these sites was undercutting, though this was difficult to objectively document (that is, with photographs) since the marsh edge was nearly always submerged.

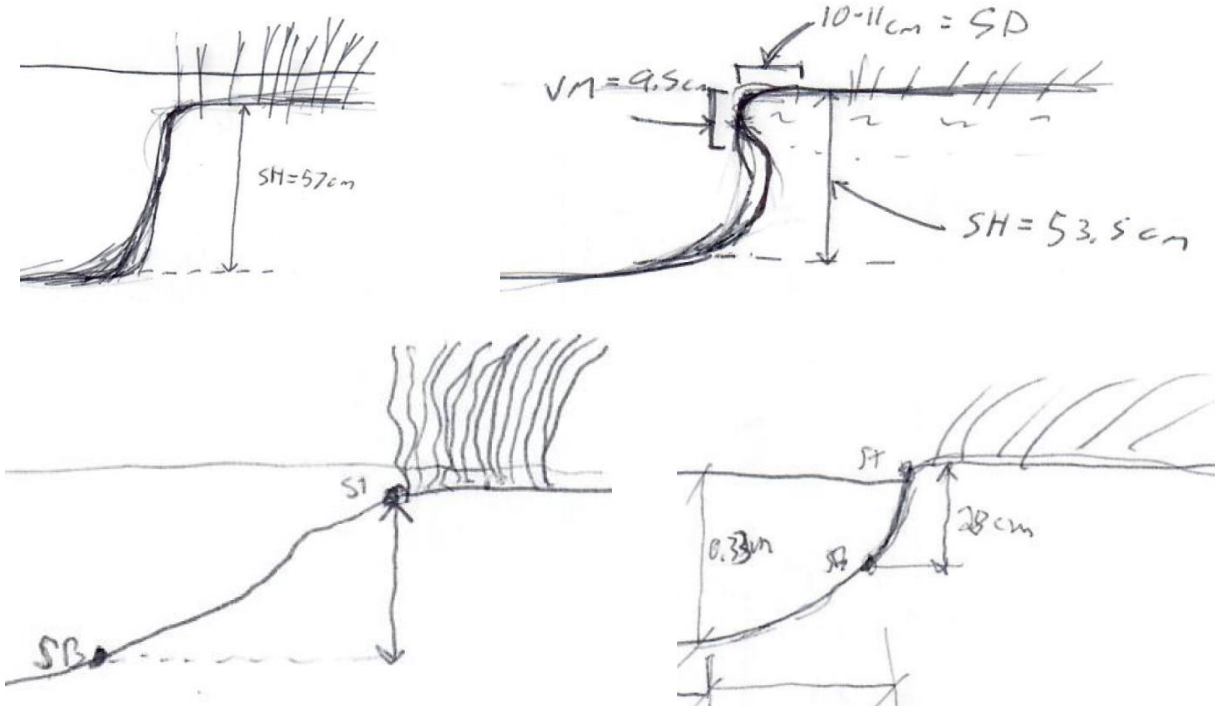

Fig. 10. Examples of scarp and marsh edge morphology observed in Terrebonne Bay

6. CONCLUSIONS

The draft of Louisiana's 2017 Coastal Master Plan (CPRA) estimates that up to an additional 1,756 m^2 of land will be lost in the next 50 years without aggressive coastal restoration and protection. A major mechanism causing a large proportion of the observed land loss is wind waves and surges attacking marsh boundaries. This process spurs a positive feedback cycle by increasing fetch and depth in a shallow coastal waterbody. This scenario is rapidly increasing rates

of marsh edge erosion in Terrebonne Bay, Barataria Bay, and Breton Sound, Louisiana (Chen et al. 2013). Therefore, a model that can confidently predict the response of a stretch of coastal marsh to a given wave climate would prove a valuable tool for the management of coastal resources to mitigate erosion hazards.

To this end, future work in Terrebonne Bay must incorporate laboratory testing on undisturbed samples collected in the field, For soil testing, 90-cm undisturbed samples will be collected in thin-walled 10-cm (4-in.) diameter aluminum tubes at each field testing location, and will be transported to LSU's Coastal Engineering Laboratory in accordance with ASTM D4220 (2014). The cores will be first run through a Geotek Multi-Sensor Core Logger (MSCL) for a rapid, continuous representation of down-core bulk-density. The bulk density is determined by both lithology and porosity, so profile comparisons can be used to correlate with the soil behavior index and moisture content measured by the SMRT-CPTu apparatus. Next, the cores will be split lengthwise for geotechnical analyses. Grain size analysis will be performed every 0.1 m down-core using a Beckman Coulter LS 13 320 Laser Diffraction Particle Size Analyzer (0.04-2000 μm). In addition, disturbed samples every 0.1 m will be tested to measure physical index tests, e.g., liquid limit (LL), plastic limit (PL), organic matter content (OMC), natural water content (w_o), salinity, root content, and mini-vane shear strength. A high pressure (i.e., 60 psi) Mark IV CSM will be employed to measure the critical shear stress at 0.1-m intervals within each core sample. Data analyses and integration of field and laboratory observations will be used to identify the ecological and geotechnical factors that influence erosional resistance and can be incorporated into the marsh edge erosion model.

These proposed laboratory measurements will also serve to validate the cone penetration test data presented in this report. Though the environmental parameters measured by the SMRT module on subsequent field investigations will likely deviate from what was previously observed, the soil stratigraphy and subsurface geotechnical properties at these locations are not expected to change drastically in such a brief timeframe. Laboratory-measured soil properties will allow our research group to calibrate our SMRT-CPTu cone for use the soil types found in coastal marsh environments and, as a result, allow us to be more effective in developing correlations between the geotechnical, hydrodynamic, and ecological factors contributing to marsh edge erosion.

REFERENCES

Allison, M., Chen, Q. J., Couvillion, B., Freeman, A., Leadon, M., McCorquidale, A., Meselhe, E., Ramatchandirane, C., Reed, D., and White, E. (2015). "2017 Coastal Master Plan: Model Improvement Plan, Attachment C3-2 – Marsh Edge Erosion." *2017 Draft Coastal Master Plan*, Coastal Protection and Restoration Authority, Baton Rouge, LA, 51.

American Society for Testing and Materials (2012). "Electronic friction cone and piezocone penetration testing of soils." *D5778*, ASTM International, West Conshohocken, PA.

American Society for Testing and Materials (2015). "Field vane shear test in saturated fine-grained soils." *D2573/D2573M*, ASTM International, West Conshohocken, PA.

Amos, C. L., Grant, J., Daborn, G. R., and Black, K. (1992). "Sea Carousel—A benthic, annular flume." *Estuarine, Coastal and Shelf Science*, 34(6), 557-577.

Are, D., Kemp, G. P., Giustina, F., Day, J., and Scarton, F. (2002). "A portable, electrically-driven Dutch cone penetrometer for geotechnical measurements in soft estuarine sediments." *Journal of Coastal Research*, 18(2), 372-378.

ASTM (2014). "Standard practices for preserving and transporting soil samples." *D4220/D4220M*, ASTM International,, West Conshohocken, PA.

Bendoni, M., Francalanci, S., Cappietti, L., and Solari, L. (2014). "On salt marshes retreat: Experiments and modeling toppling failures induced by wind waves." *J. Geophys. Res.*, 119(3), 603-620.

Bendoni, M., Mel, R., Solari, L., Lanzoni, S., Francalanci, S., and Oumeraci, H. (2016). "Insights into lateral marsh retreat mechanism through localized field measurements." *Water Resour. Res.*, 52(2), 1146-1464.

Black, K., Tolhurst, T. J., Paterson, D. M., and Hagerthey, S. E. (2002). "Working with natural cohesive sediments." *Journal of Hydraulic Engineering*, 128(1), 2-8.

Briaud, J.-L., Li, Y., and Rhee, K. (2006). "BCD: A soil modulus device for compaction control." *Journal of Geotechnical and Geoenvironmental Engineering*, 132(1), 108-115.

Chen, Q., Ozeren, Y., Zhang, G., Wren, D., Wu, W., Jadhav, R., Parker, K., and Pant, H. (2013). "Laboratory and field investigations of marsh edge erosion." *Sediment Transport: Monitoring, Modeling and Management*, A. A. Khan, and W. Wu, eds., Nova Science Publishers, 311-337.

Chen, Q., Zhao, H., Hu, K., and Douglass, S. L. (2005). "Prediction of wind waves in a shallow estuary." *Journal of Waterway, Port, Coastal, and Ocean Engineering*, 131(4), 137-148.

Couvillion, B. R., Barras, J. A., Steyer, G. D., Sleavin, W., Fischer, M., Beck, H., Trahan, N., Griffin, B., and Heckman, D. (2011). "Land area change in coastal Louisiana from 1932 to 2010." *National Wetlands Research Center*, USGS, Lafayette, LA.

CPRA (2012). *2012 Coastal Master Plan*, Coastal Protection and Restoration Authority, Baton Rouge, LA.

CPRA (2015). *Louisiana Flood Protection Design Guidelines (LFPDG) – Geotechnical Section*, Coastal Protection and Restoration Authority, Baton Rouge, LA.

CPRA (2017). *2017 Draft Coastal Master Plan*, Coastal Protection and Restoration Authority, Baton Rouge, LA.

CPRA (2017). "Coastwide Reference Monitoring System-Wetlands Monitoring Data."Baton Rouge, LA.

D'Alpaos, A., Lanzoni, S., Marani, M., and Rinaldo, A. (2007). "Landscape evolution in tidal embayments: Modeling the interplay of erosion, sedimentation, and vegetation dynamics." *Journal of Geophysical Research*, 112(F1).

Day, J. W., Kemp, G. P., Reed, D. J., Cahoon, D. R., Boumans, R. M., Suhayda, J. M., and Gambrell, R. (2011). "Vegetation death and rapid loss of surface elevation in two contrasting Mississippi Delta salt marshes: The role of sedimentation, autocompaction and sea-level rise." *Ecol. Eng.*, 37(2), 229-240.

Feagin, R. A., Lozada-Bernard, S. M., Ravens, T. M., Möller, I., Yeager, K. M., and Baird, A. H. (2009). "Does vegetation prevent wave erosion of salt marsh edges?" *Proc. Natl. Acad. Sci. U.S.A.*, 106(25), 10109-10113.

Gabet, E. J. (1998). "Lateral migration and bank erosion in a saltmarsh tidal channel in San Francisco Bay, California." *Estuaries*, 21(4), 745-753.

Gedan, K. B., Silliman, B. R., and Bertness, M. D. (2009). "Centuries of human-driven change in salt marsh ecosystems." *Ann Rev Mar Sci*, 1, 117-141.

Howes, N. C., FitzGerald, D. M., Hughes, Z. J., Georgiou, I. Y., Kulp, M. A., Miner, M. D., Smith, J. M., and Barras, J. A. (2010). "Hurricane-induced failure of low salinity wetlands." *Proc. Natl. Acad. Sci. U.S.A.*, 107(32), 14014-14019.

Johnson, C. L. (2016). "The influence of soil properties on marsh edge erosion." M.S.C.E. master's thesis, Louisiana State Univ., Baton Rouge, LA.

Knutson, P. L. (1987). "Role of coastal marshes in energy dissipation and shore protection." *The Ecology and Management of Wetlands*, D. D. Hook, W. H. McKee, Jr., H. K. Smith, J. Gregory, V. G. Burrell, Jr., M. R. DeVoe, R. E. Sojka, S. Gilbert, R. Banks, L. H. Stolzy, C. Brooks, T. D. Matthews, and T. H. Shear, eds., Timber Press, Portland, OR, 161-175.

Leonardi, N., and Fagherazzi, S. (2015). "Effect of local variability in erosional resistance on large scale morphodynamic response of salt marshes to wind waves and extreme events." *Geophysical Research Letters*, 42(14), 5872-5879.

Lo, E. L., Bentley, S. J., and Xu, K. (2014). "Experimental study of cohesive sediment consolidation and resuspension identifies approaches for coastal restoration: Lake Lery, Louisiana." *Geo-Marine Letters*, 34(6), 499-509.

Marani, M., D'Alpaos, A., Lanzoni, S., and Santalucia, M. (2011). "Understanding and predicting wave erosion of marsh edges." *Geophysical Research Letters*, 38(21), L21401.

Mariotti, G., and Fagherazzi, S. (2010). "A numerical model for the coupled long-term evolution of salt marshes and tidal flats." *Journal of Geophysical Research*, 115(F1).

Morgenstern, N. R., and Price, V. E. (1965). "The analysis of the stability of general slip surface." *Géotechnique*, 15(1), 79-93.

Parker, K. R. (2014). "Field and numerical investigation of wave power and shoreline retreat in Terrebonne Bay, Southern Louisiana." M.S.C.E. master's thesis, Louisiana State Univ., Baton Rouge, LA.

Penland, S., Wayne, L., Britsch, L. D., Williams, S. J., Beall, A. D., and Butterworth, V. C. (2000). "Process classification of coastal land loss between 1932 and 1990 in the Mississippi River Delta Plain, Southeastern Louisiana." U.S. Geological Survey, Woods Hole, MA.

Pestrong, R. (1972). "Tidal-flat sedimentation at Cooley Landing, Southwest San Francisco Bay." *Sediment. Geol.*, 8(4), 251-288.

Pollen-Bankhead, N., and Simon, A. (2009). "Enhanced application of root-reinforcement algorithms for bank-stability modeling." *Earth Surface Processes and Landforms*, 34(4), 471-480.

Pollen-Bankhead, N., and Simon, A. (2010). "Hydrologic and hydraulic effects of riparian root networks on streambank stability: Is mechanical root-reinforcement the whole story?" *Geomorphology*, 116(3-4), 353-362.

Priestas, A., Mariotti, G., Leonardi, N., and Fagherazzi, S. (2015). "Coupled Wave Energy and Erosion Dynamics along a Salt Marsh Boundary, Hog Island Bay, Virginia, USA." *Journal of Marine Science and Engineering*, 3(3), 1041-1065.

Redfield, A. C. (1972). "Development of a New England salt marsh." *Ecol. Monogr.*, 42(2), 201-237.

Robertson, P. K. (2009). "Interpretation of cone penetration tests – A unified approach." *Canadian Geotechnical Journal*, 14(4), 465-481.

Sasser, C. E., Evers-Hebert, E., Milan, B., and Holm, G. O., Jr. (2013). "Relationships of marsh soil strength to vegetation biomass." Coastal Protection and Restoration Authority, Baton Rouge, LA, 73.

Schwimmer, R. A. (2001). "Rates and processes of marsh shoreline erosion in Rehoboth Bay, Deleware, U.S.A." *Journal of Coastal Research*, 17(3), 672-683.

Simon, A., Curini, A., Darby, S. E., and Langendoen, E. J. (2000). "Bank and near-bank processes in an incised channel." *Geomorphology*, 35(3-4), 193-217.

Singh, A., Fienberg, K., Jerolmack, D. J., Marr, J., and Foufoula-Georgiou, E. (2009). "Experimental evidence for statistical scaling and intermittency in sediment transport rates." *Journal of Geophysical Research*, 114(F1), F01025.

Thorne, C. R., and Tovey, N. K. (1981). "Stability of composite river banks." *Earth Surface Processes and Landforms*, 6(5), 469-484.

Topp, G. C., Davis, J. L., and Annan, A. P. (1980). "Electromagnetic determination of soil water content: Measurements in coaxial transmission lines." *Water Resour. Res.*, 16(3), 574-582.

Turner, R. E. (2010). "Beneath the salt marsh canopy: Loss of soil strength with increasing nutrient loads." *Estuaries and Coasts*, 34(5), 1084-1093.

Wilson, C. A., and Allison, M. A. (2008). "An equilibrium profile model for retreating marsh shorelines in southeast Louisiana." *Estuarine, Coastal and Shelf Science*, 80(4), 483-494.

Wilson, C. A., Hughes, Z. J., and Fitzgerald, D. M. (2012). "The effects of crab bioturbation on Mid-Atlantic saltmarsh tidal creek extension: Geotechnical and geochemical changes." *Estuarine, Coastal and Shelf Science*, 106, 33-44.

Young, I. R., and Verhagen, L. A. (1996). "The growth of fetch limited waves in water of finite depth. Part 1. Total energy and peak frequency." *Coastal Engineering*, 29(1-2), 47-78.

APPENDIX

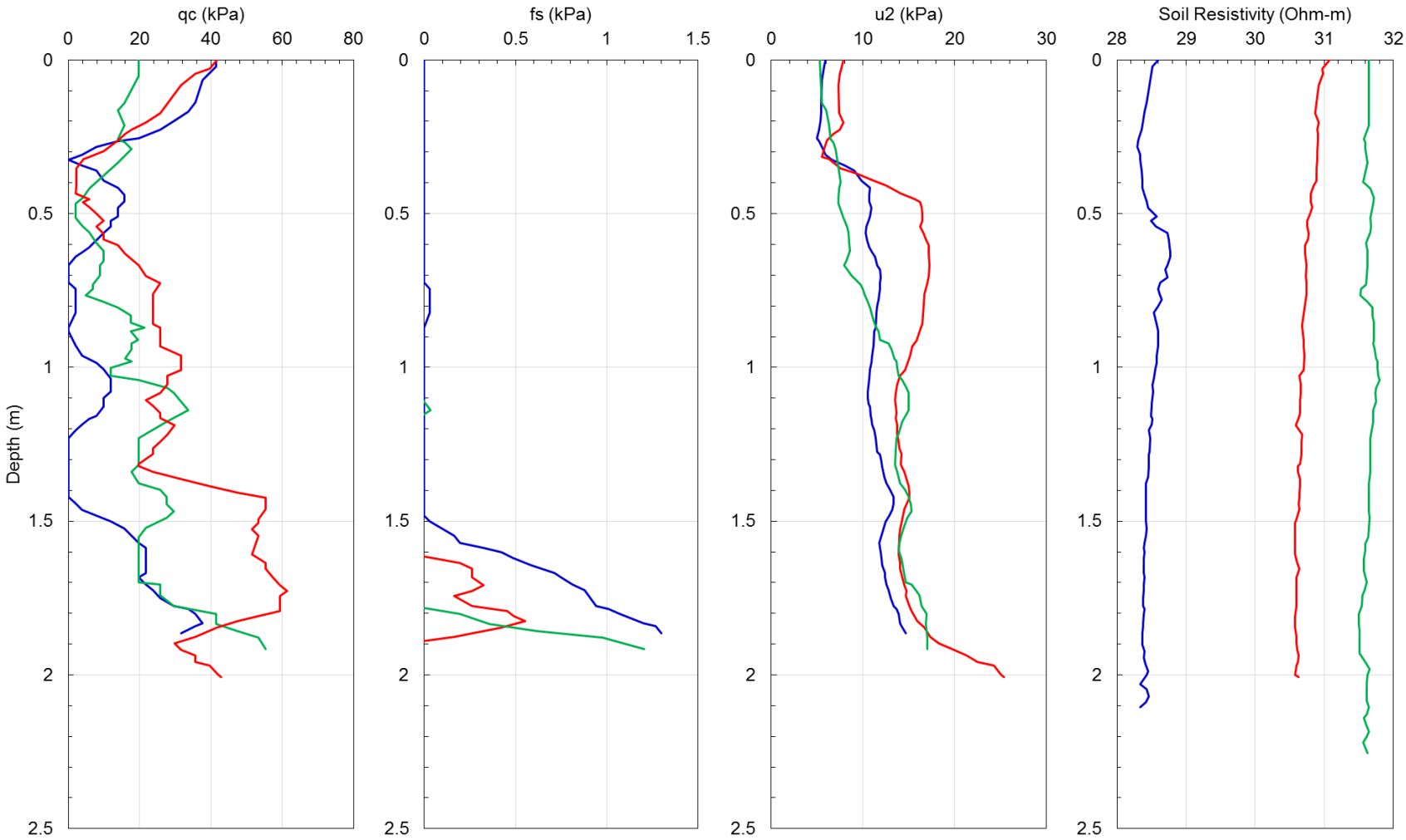

Fig. A1. CPTu soundings from Location 1, Site 3

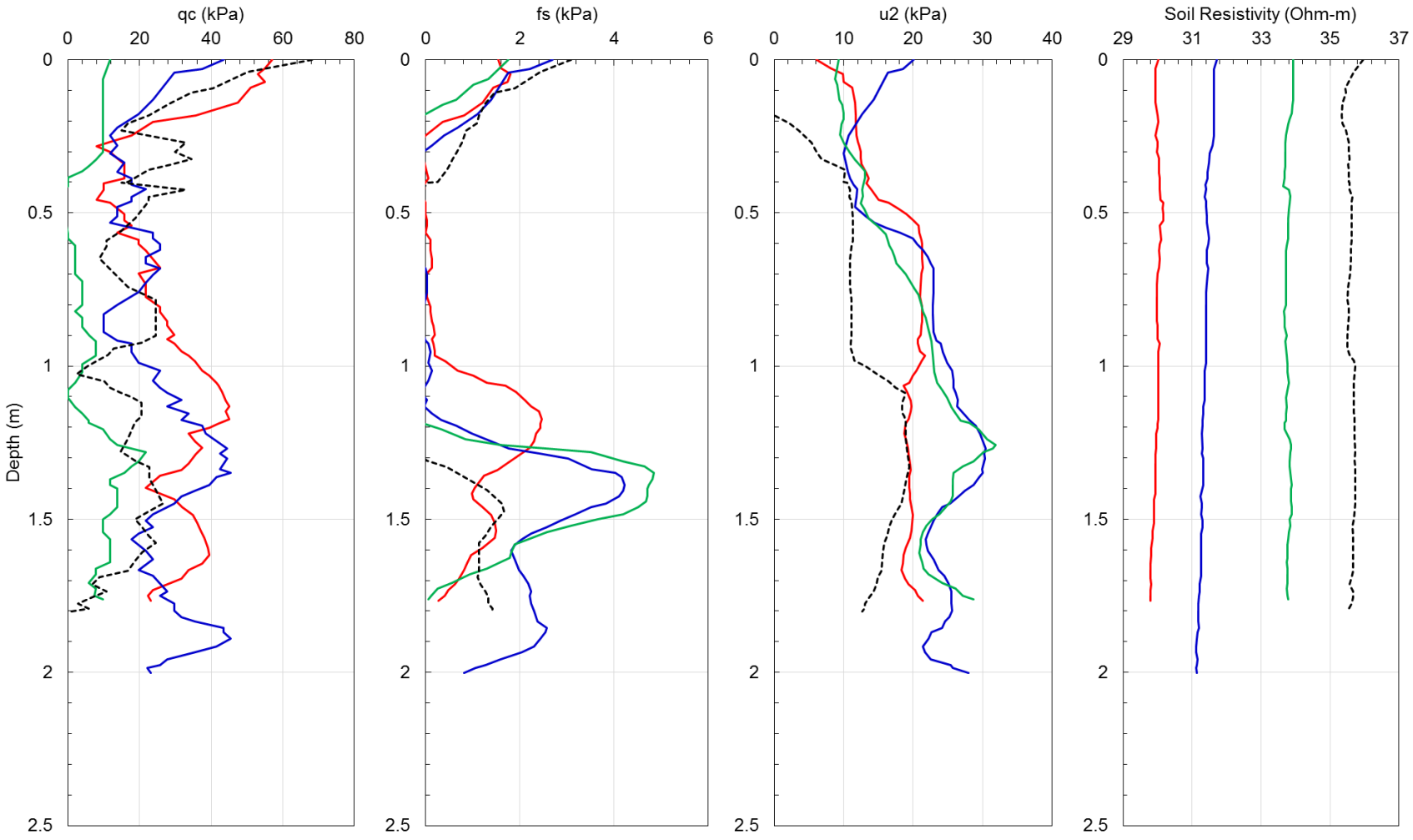

Fig. A2. CPTu soundings from Location 2, Site 3

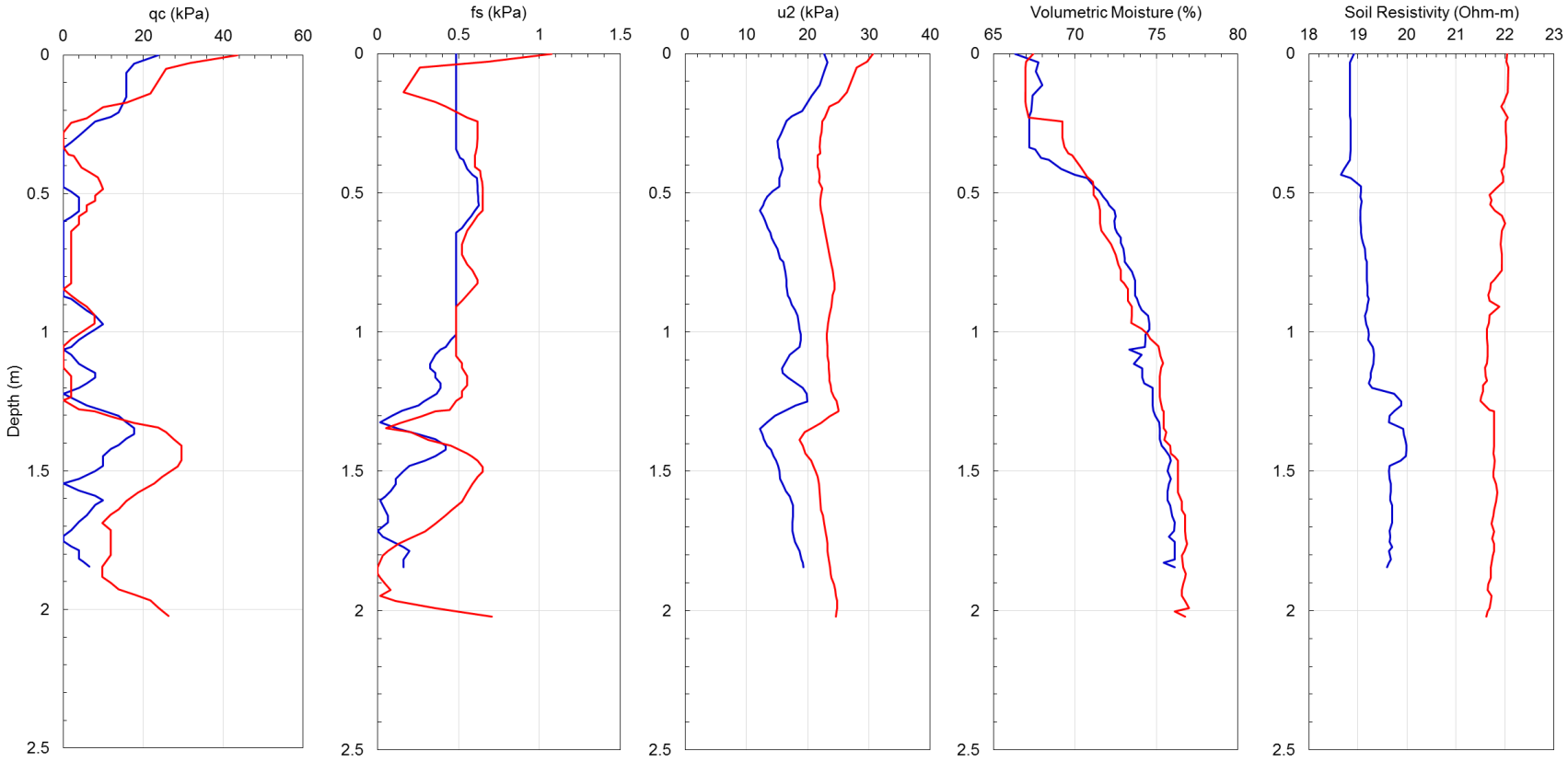

Fig. A3. CPTu soundings from Location 3, Site 3

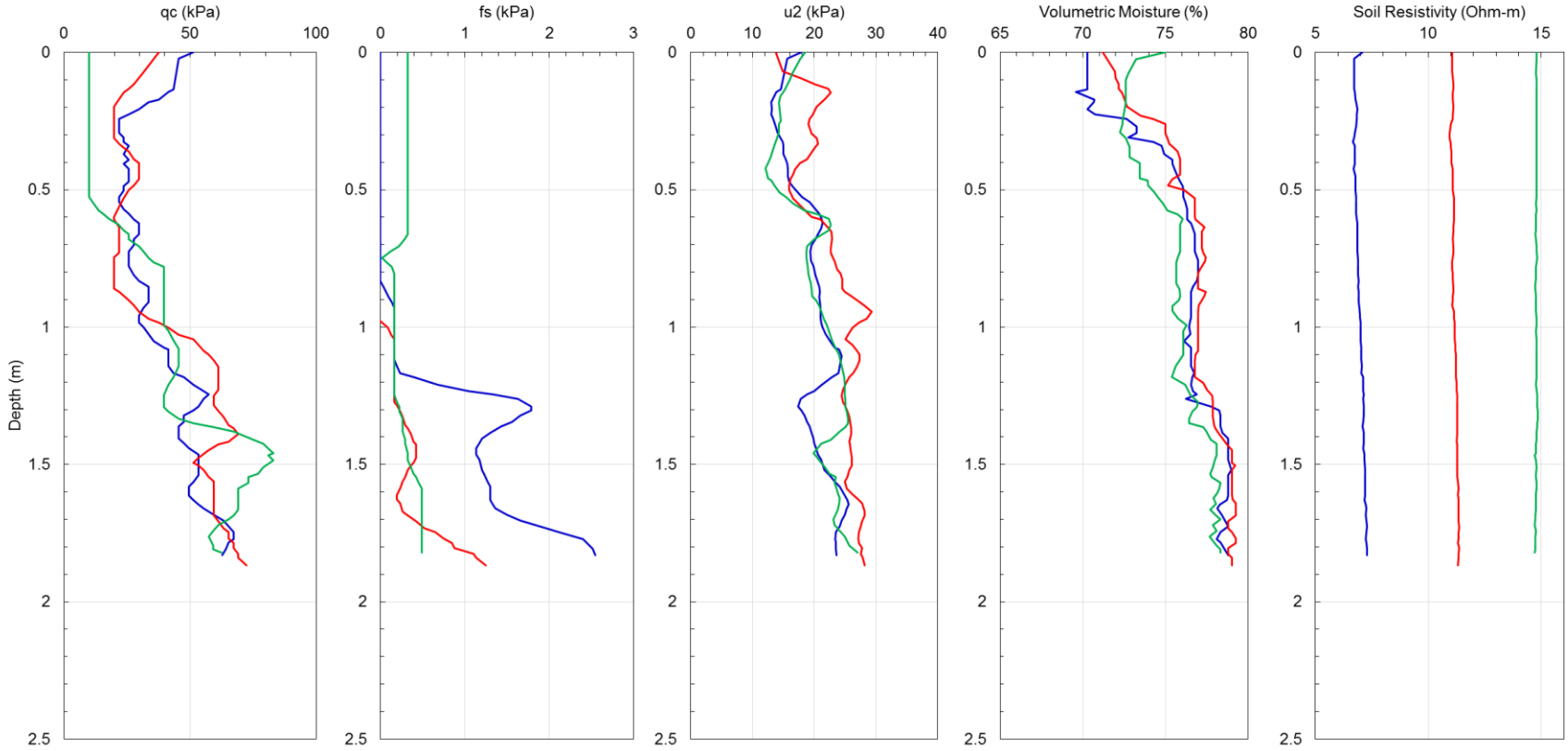

Fig. A4. CPTu soundings from Location 4, Site 3

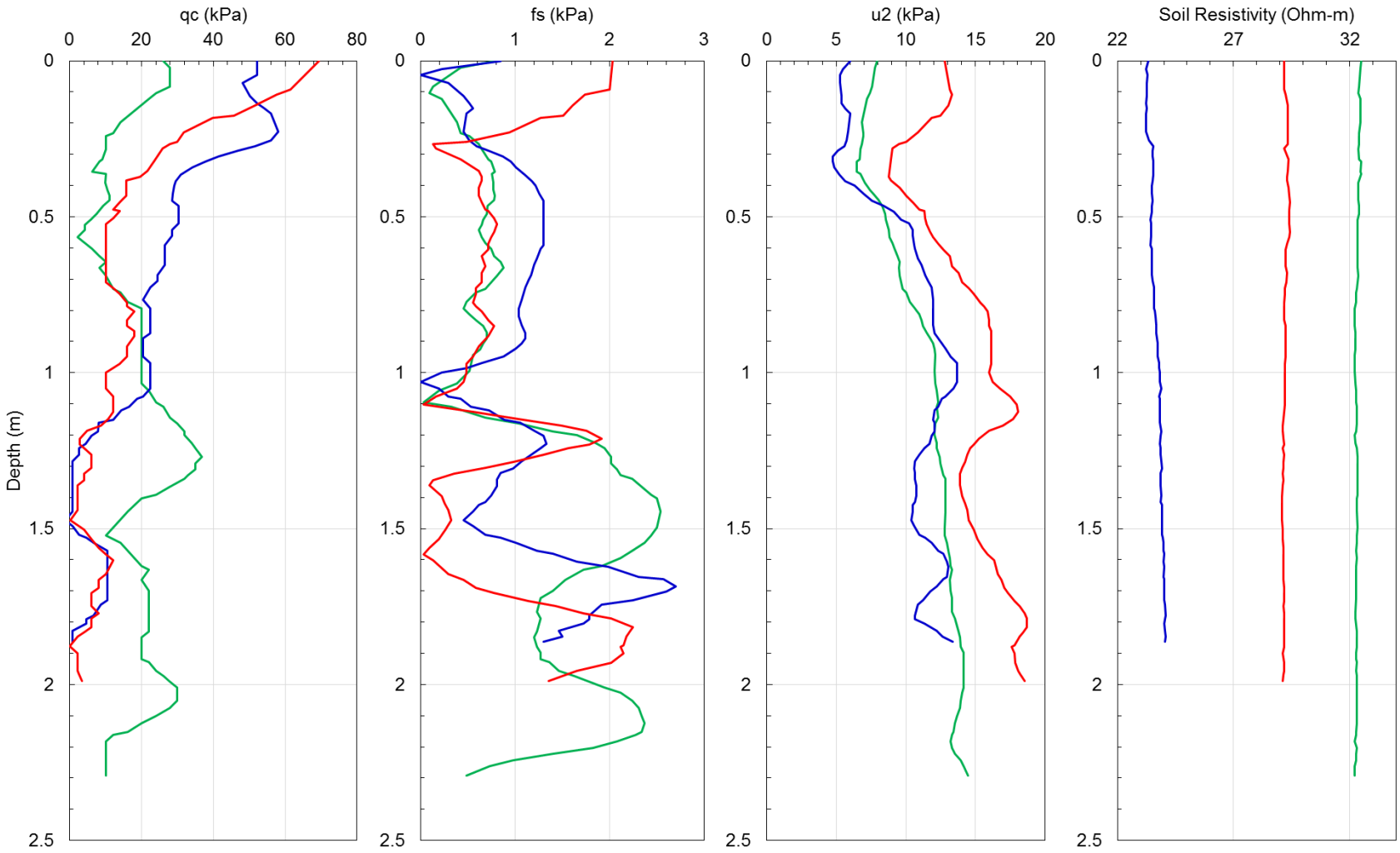

Fig. A5. CPTu soundings from Location 5, Site 3

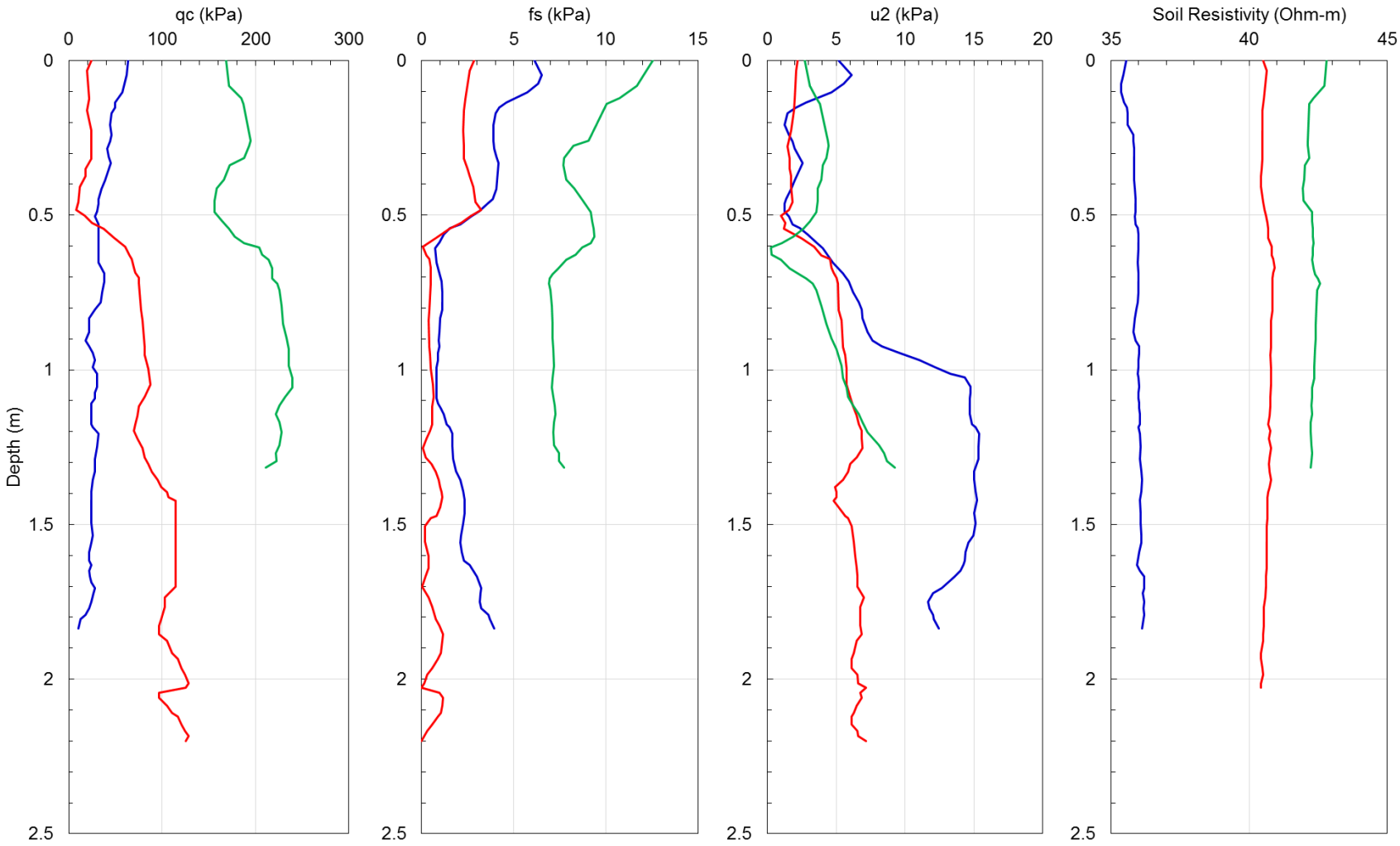

Fig. A6. CPTu soundings from Location 6, Site 3

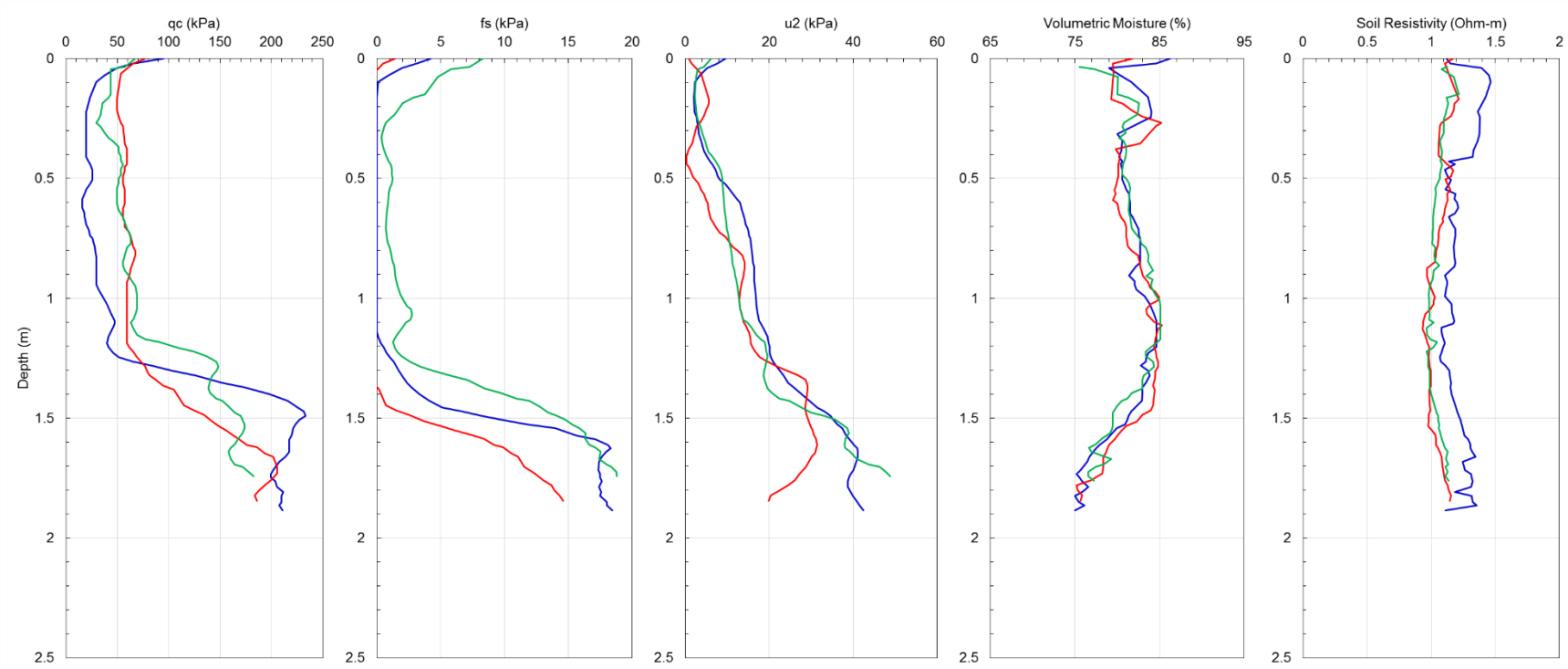

Fig. A7. CPTu soundings from Location 1, Site 2

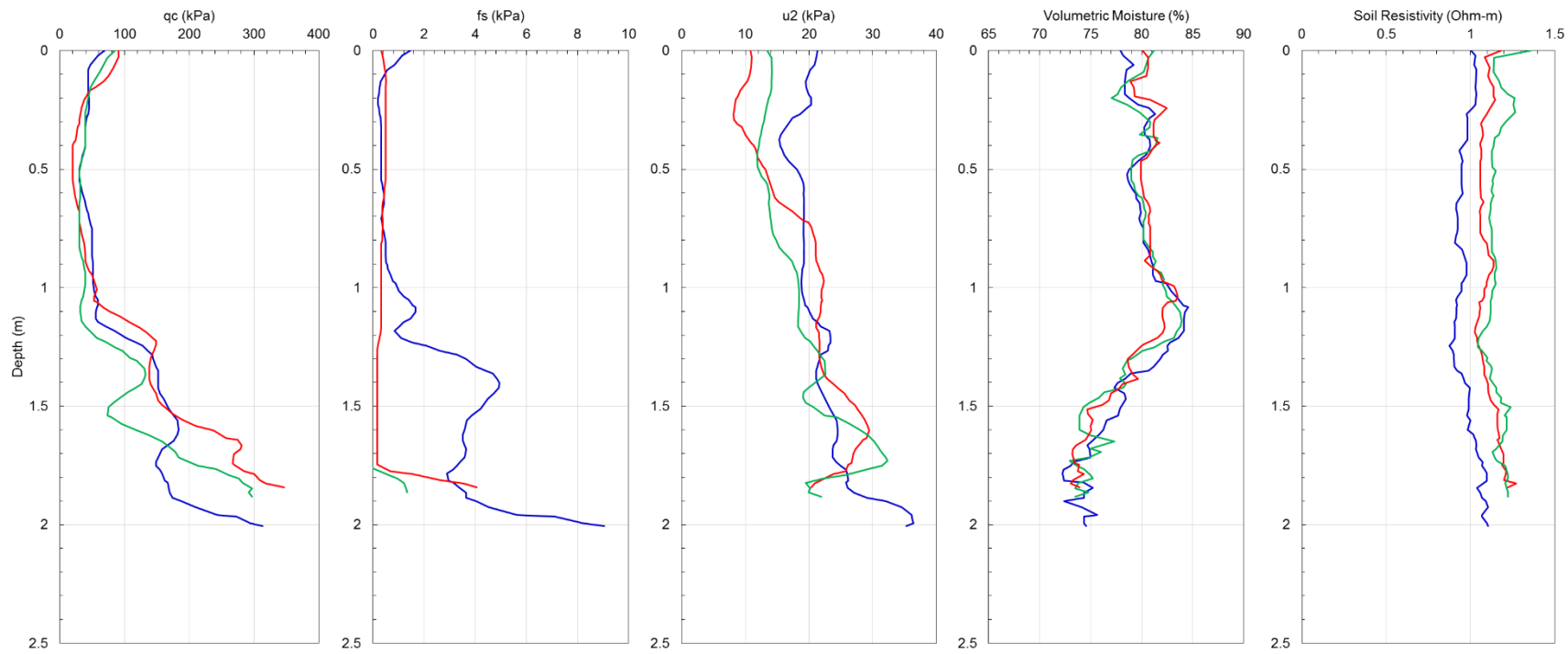

Fig. A8. CPTu soundings from Location 2, Site 2

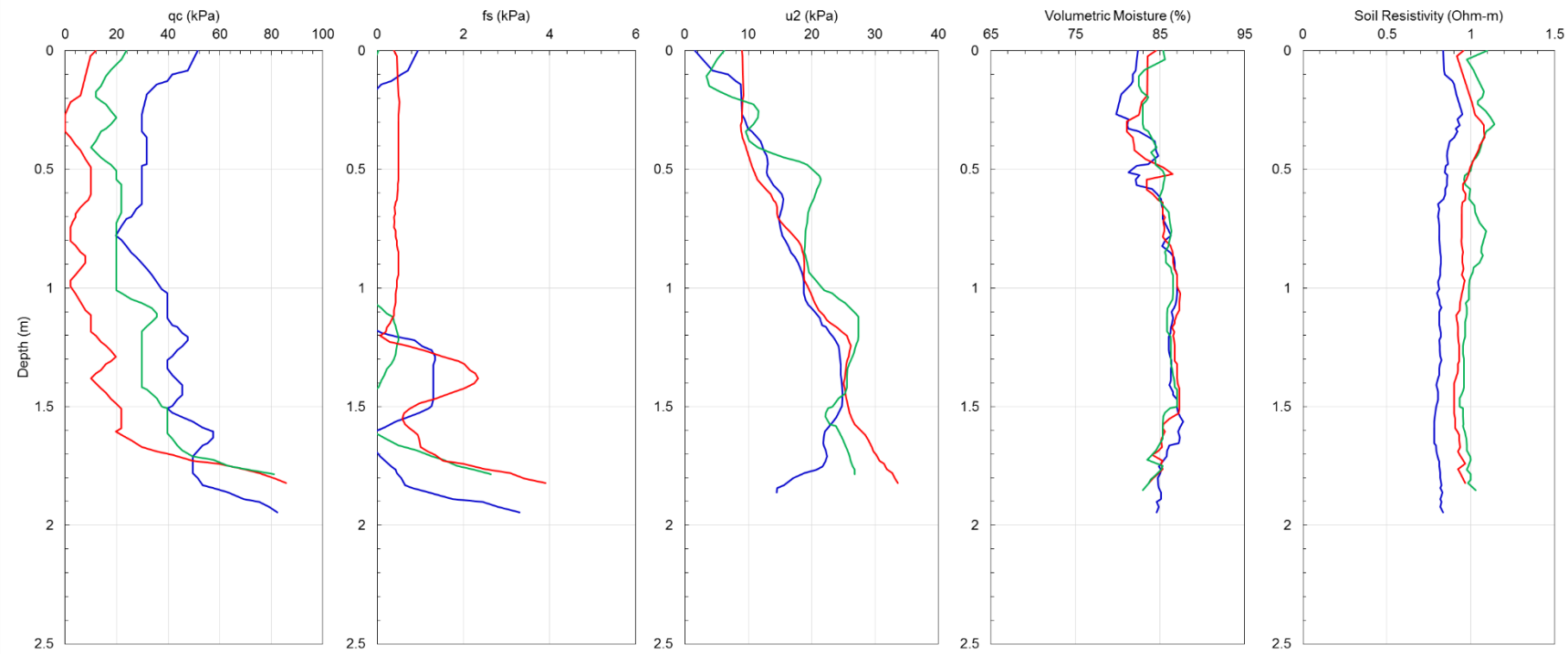

Fig. A9. CPTu soundings from Location 3, Site 2

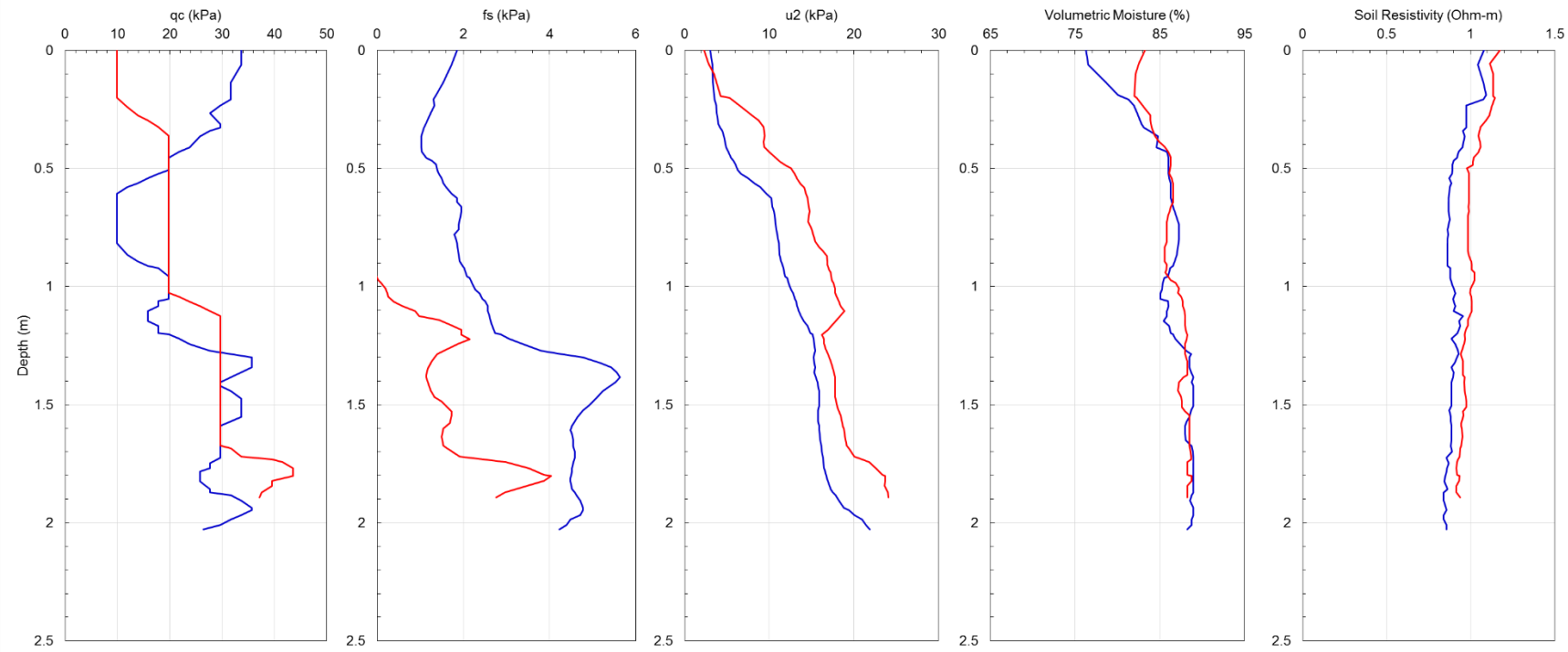

Fig. A10. CPTu soundings from Location 4, Site 2

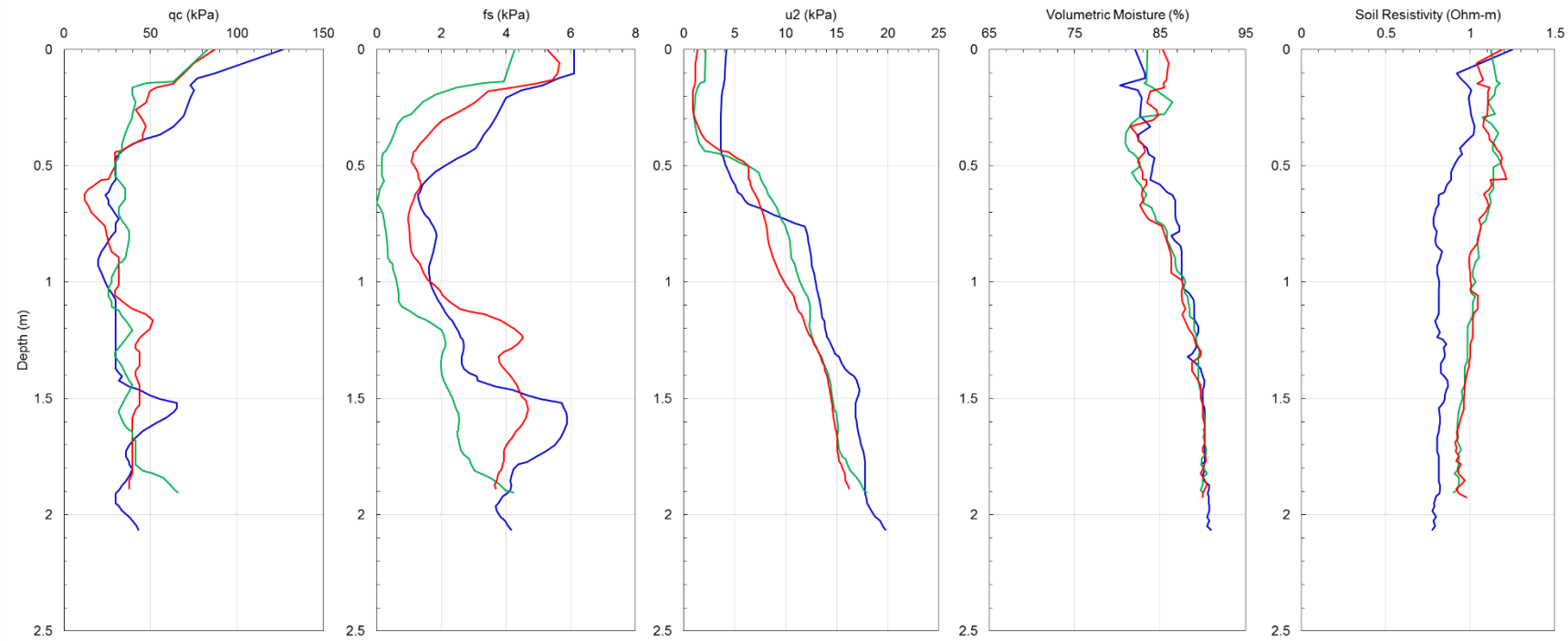

Fig. A11. CPTu soundings from Location 5, Site 2

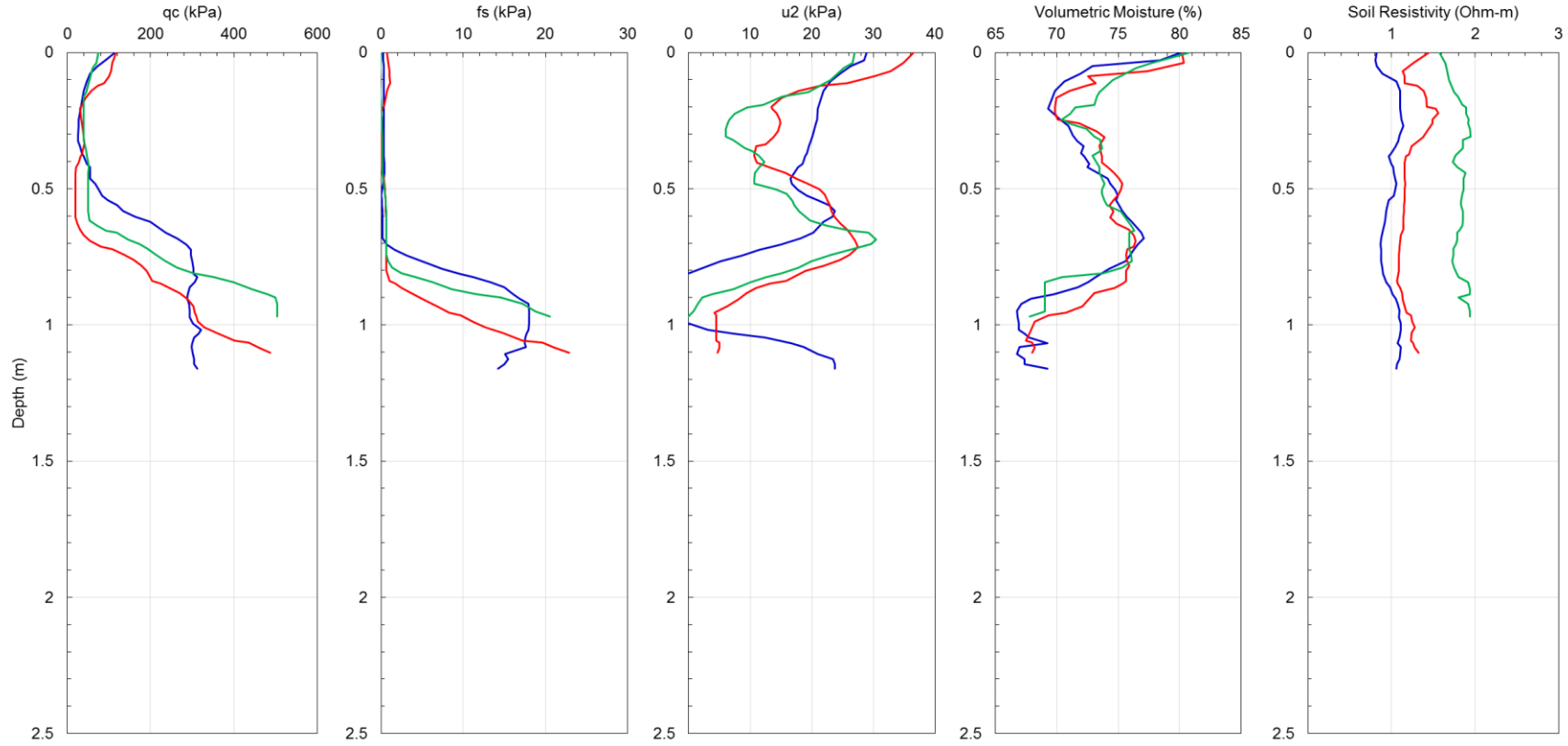

Fig. A12. CPTu soundings from Location 1, Site 1

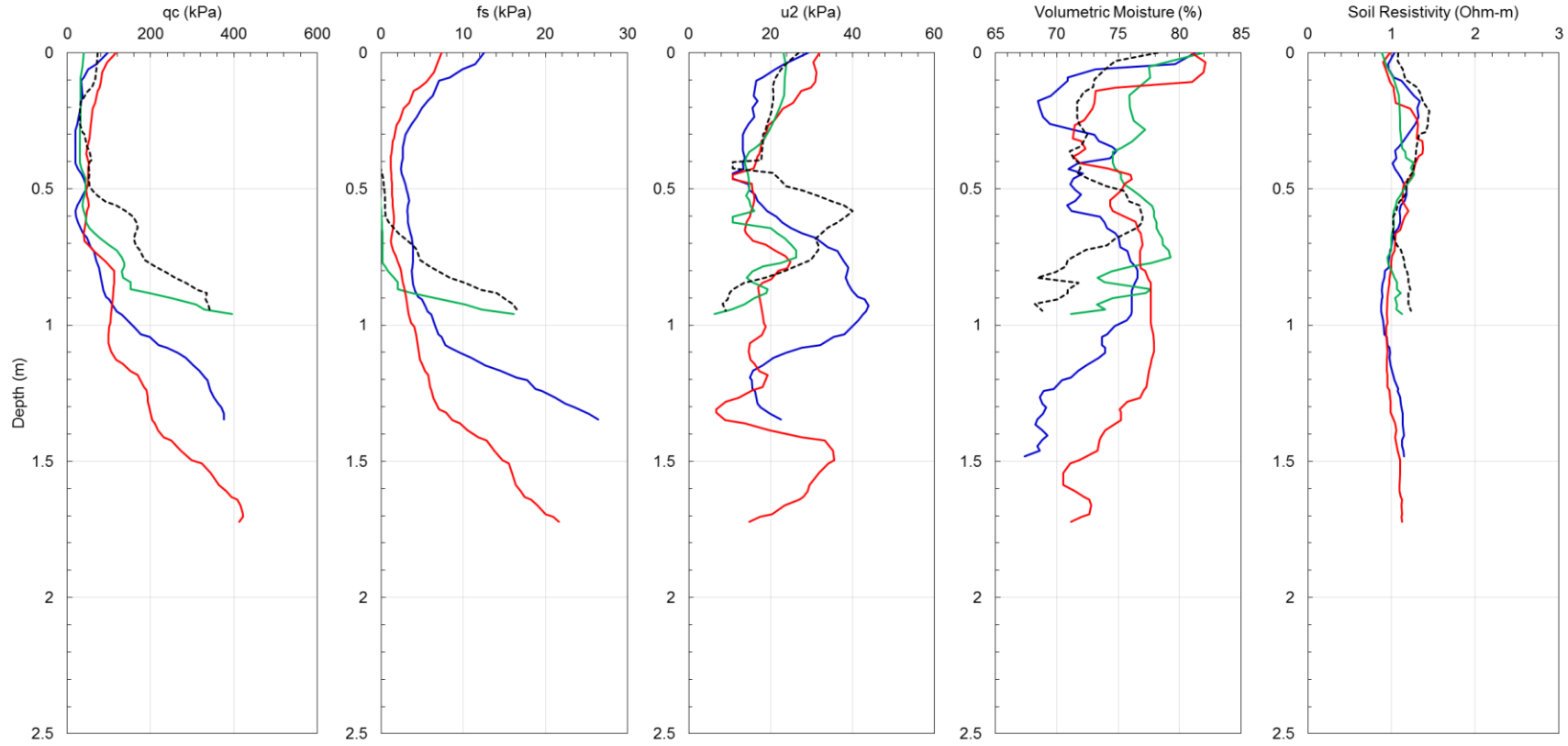

Fig. A13. CPTu soundings from Location 2, Site 1

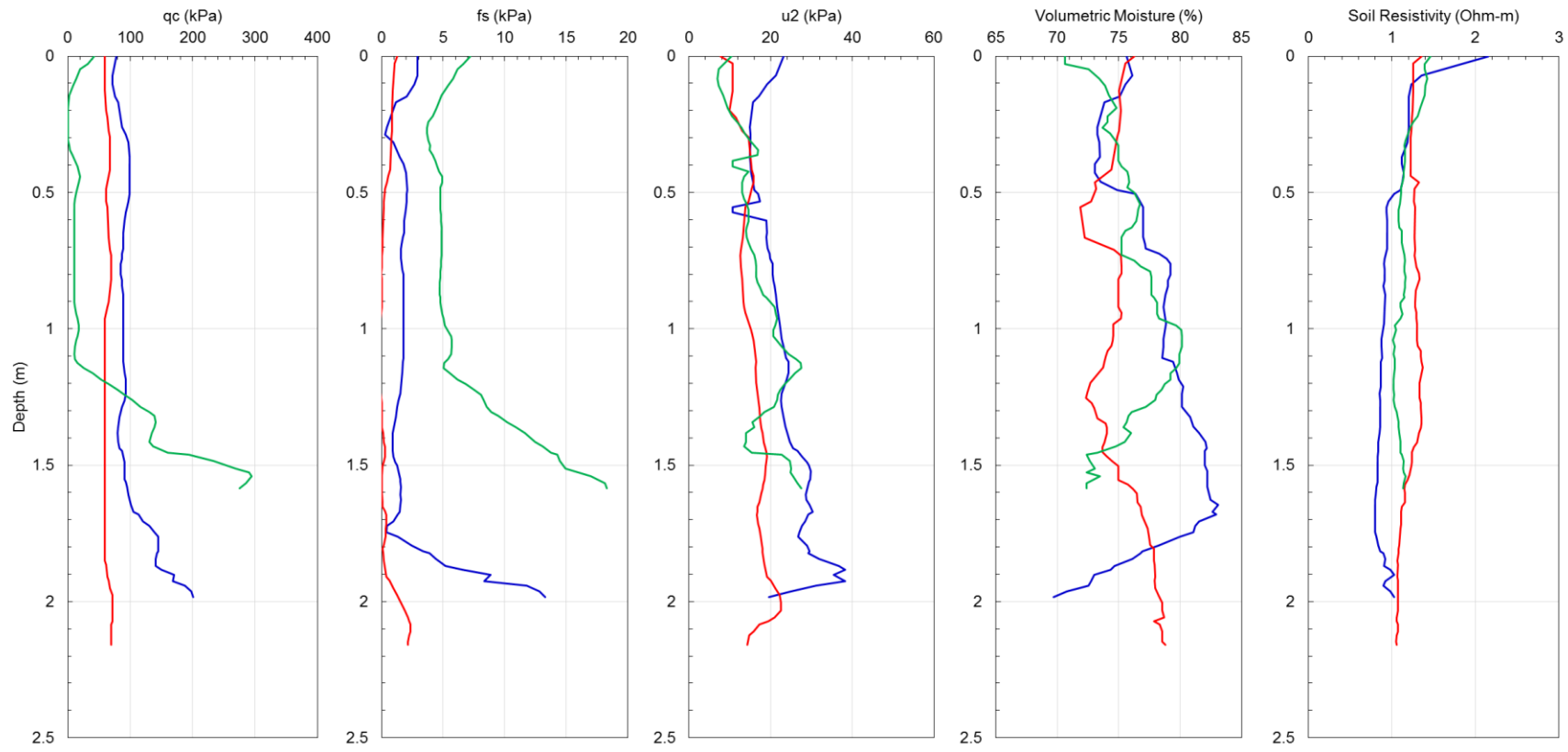

Fig. A14. CPTu soundings from Location 3, Site 1

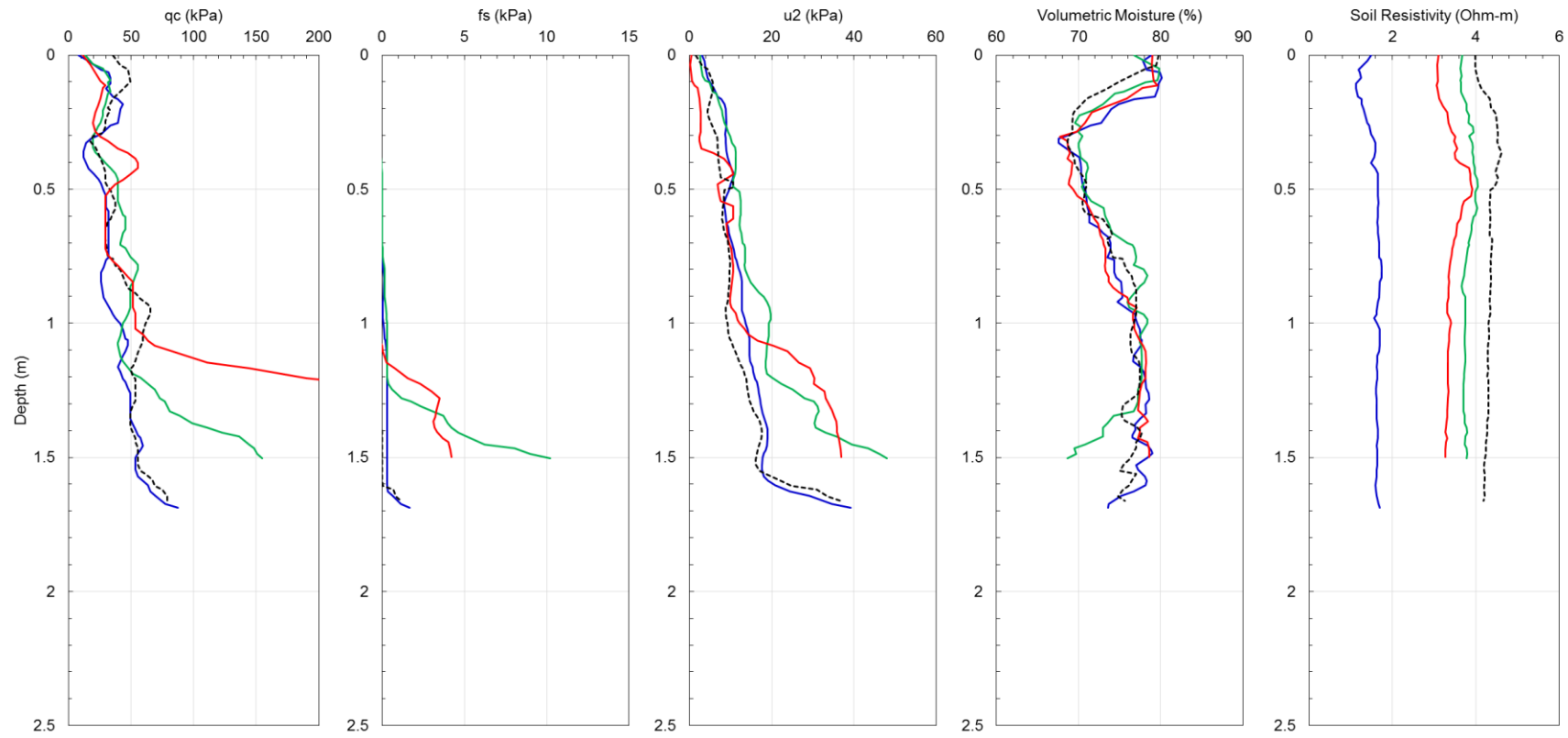

Fig. A15. CPTu soundings from Location 4, Site 1

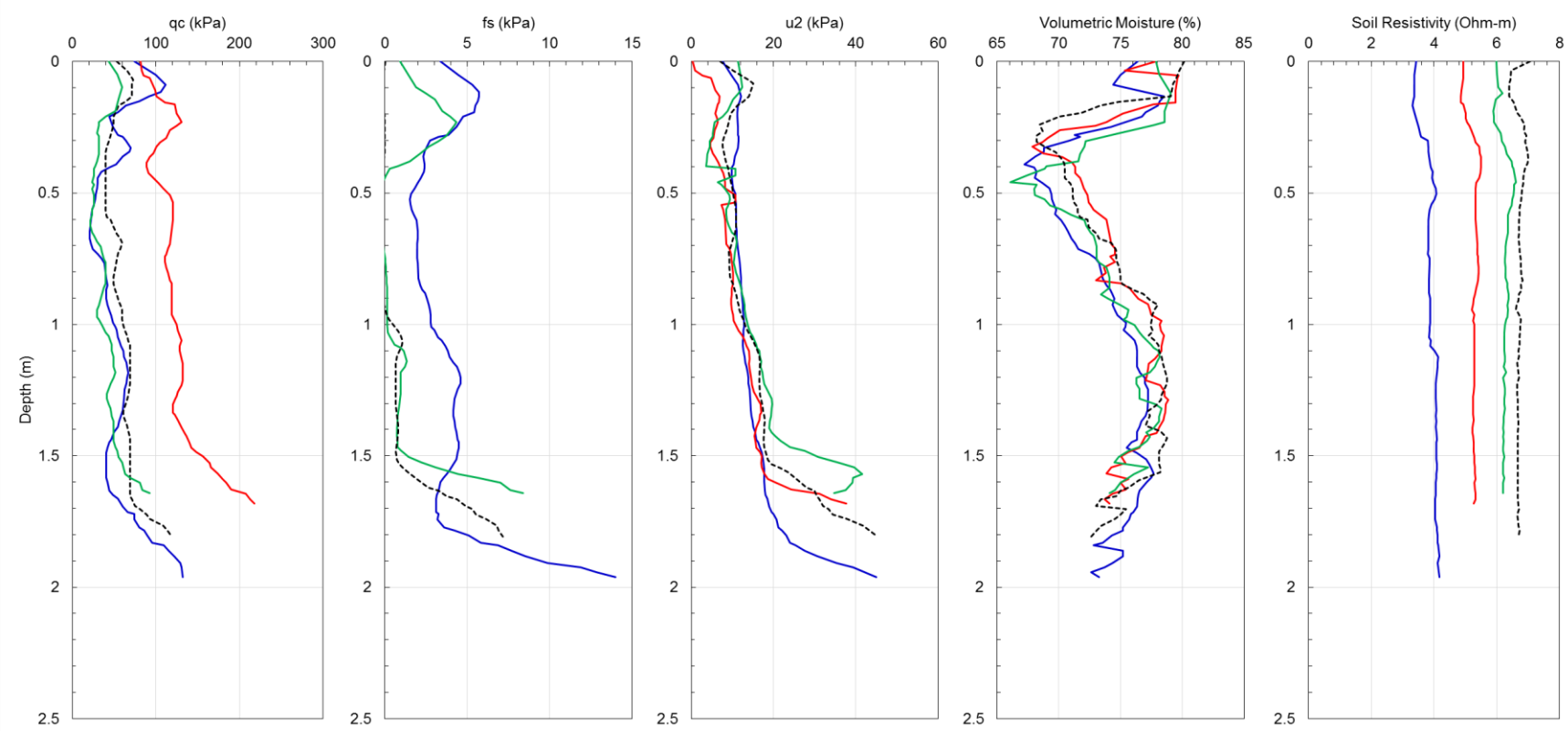

Fig. A16. CPTu soundings from Location 5, Site 1

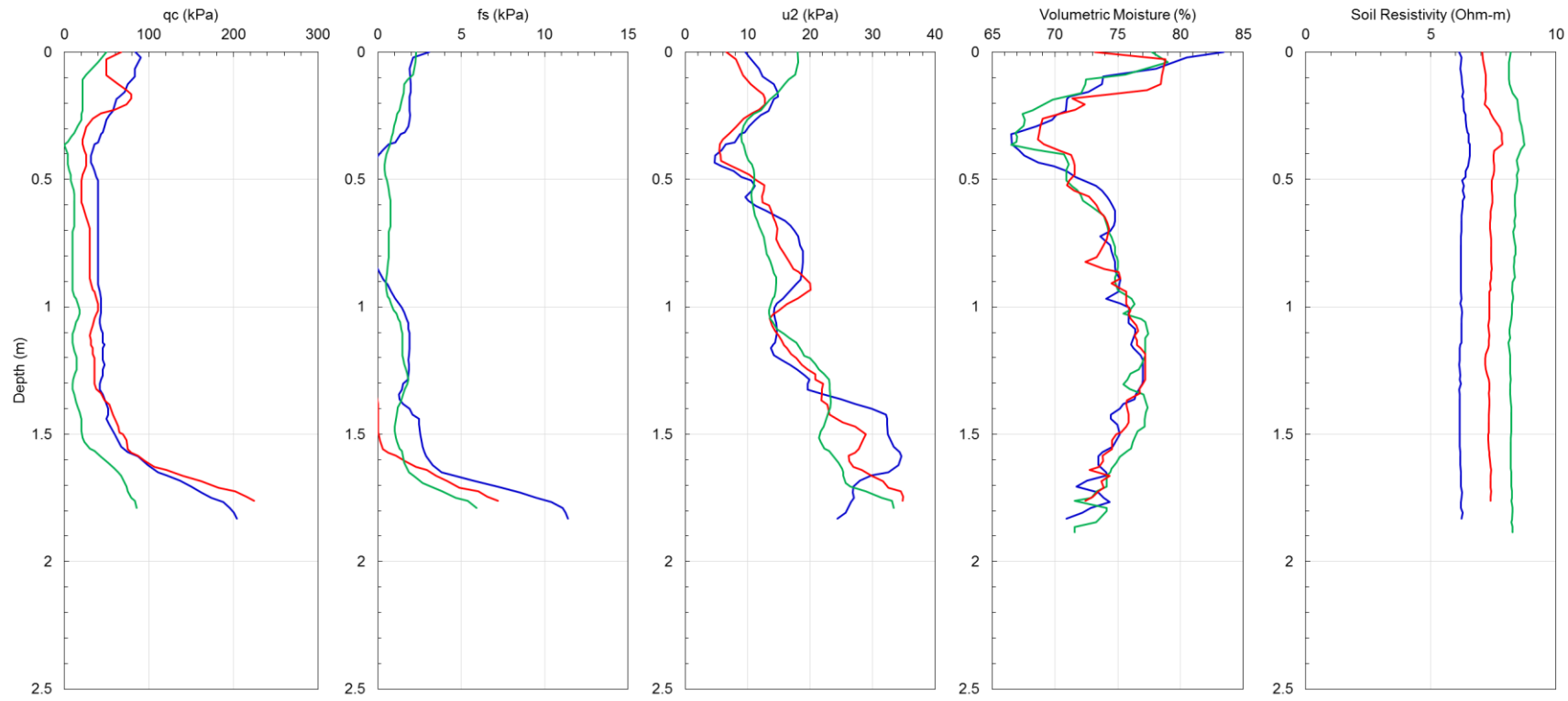

Fig. A17. CPTu soundings from Location 6, Site 1

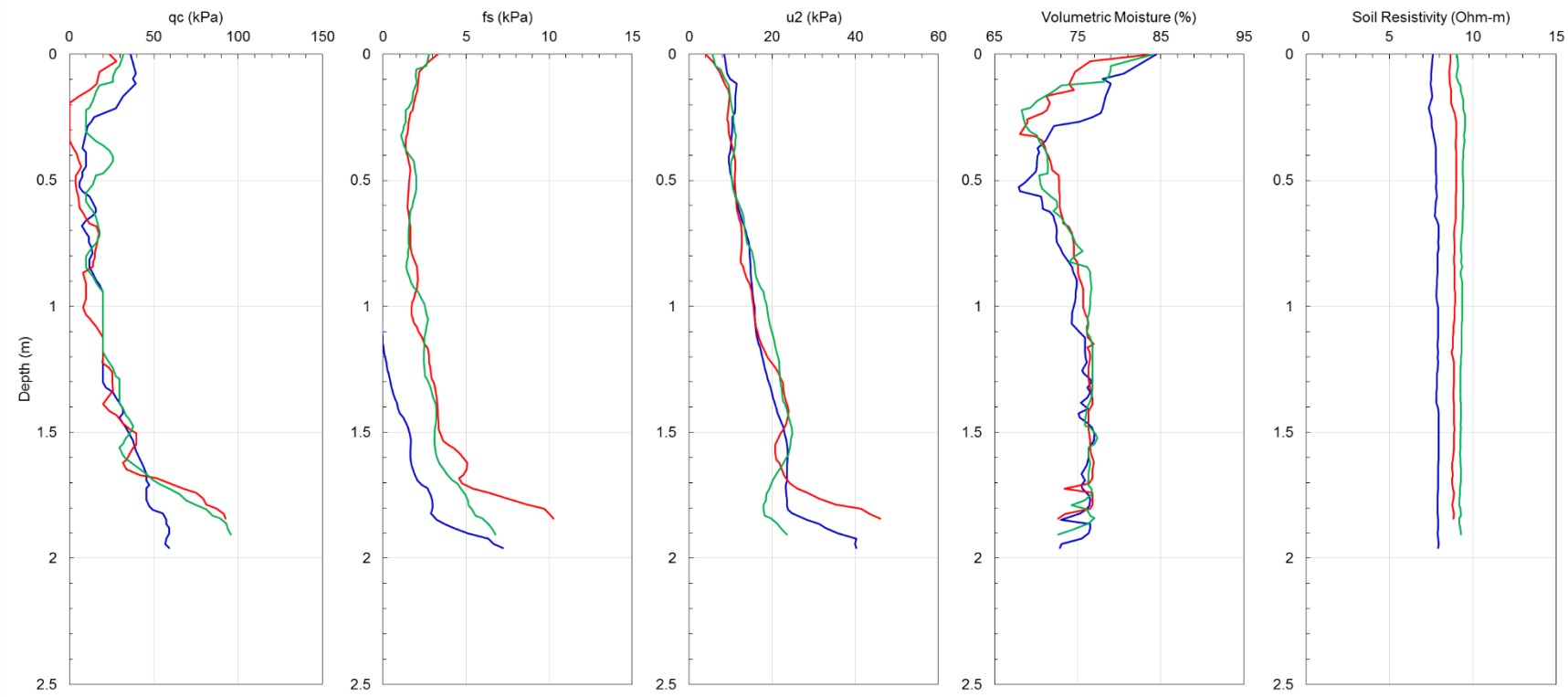

Fig. A18. CPTu soundings from Location 7, Site 1

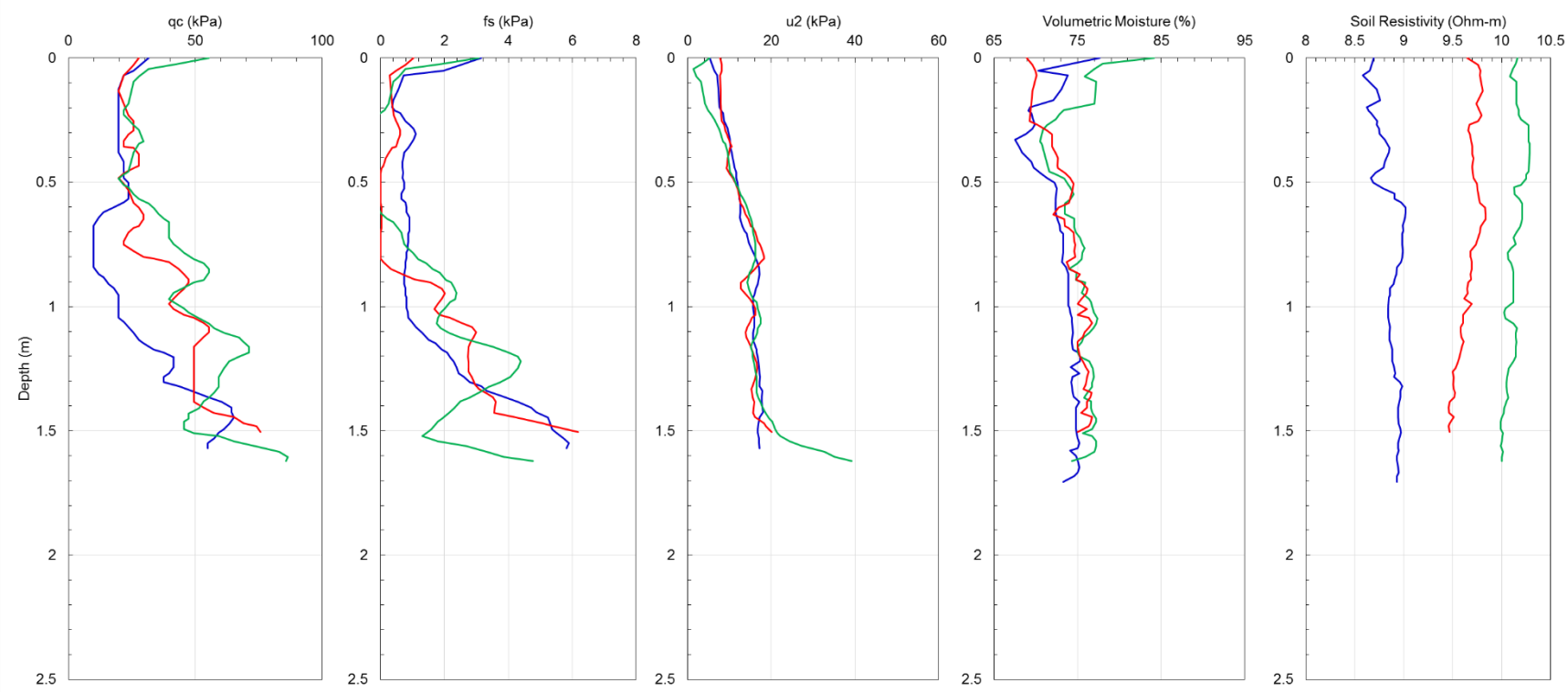

Fig. A19. CPTu soundings from Location 8, Site 1

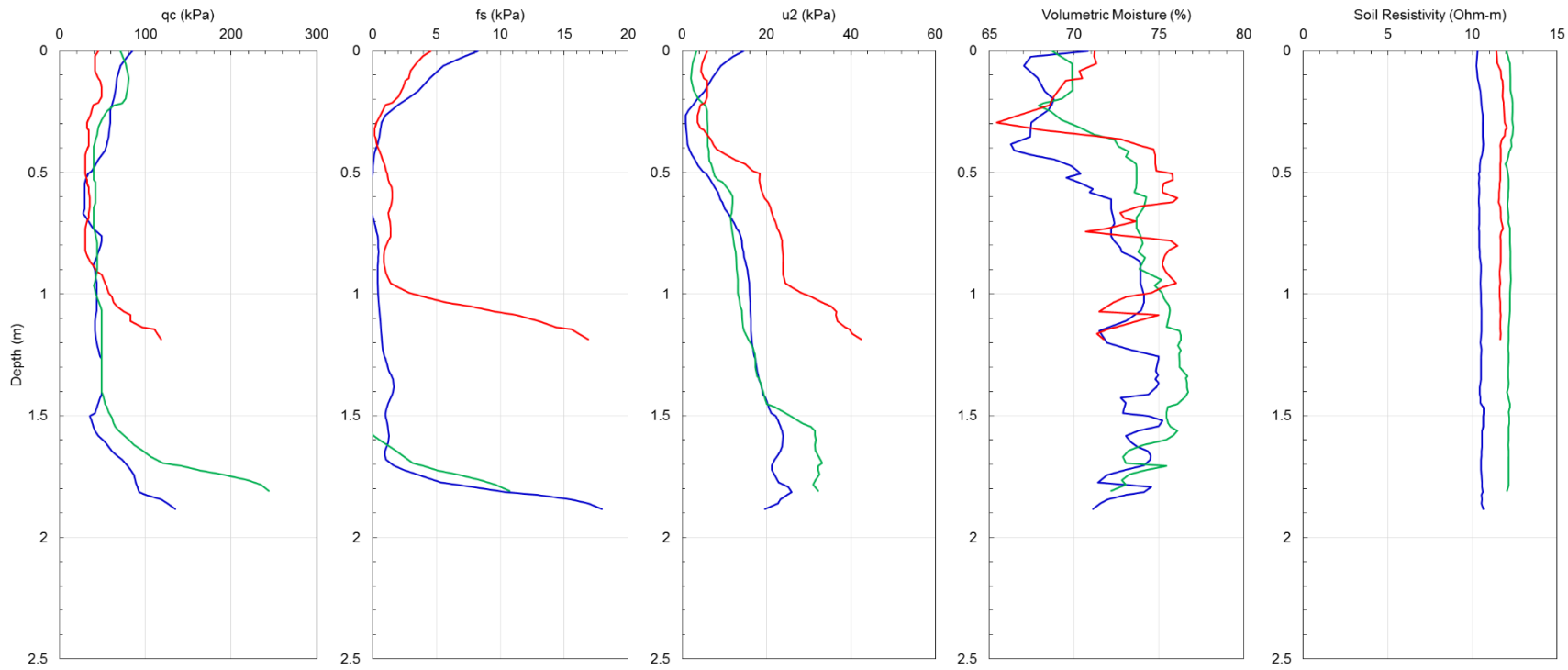

Fig. A20. CPTu soundings from Location 9, Site 1

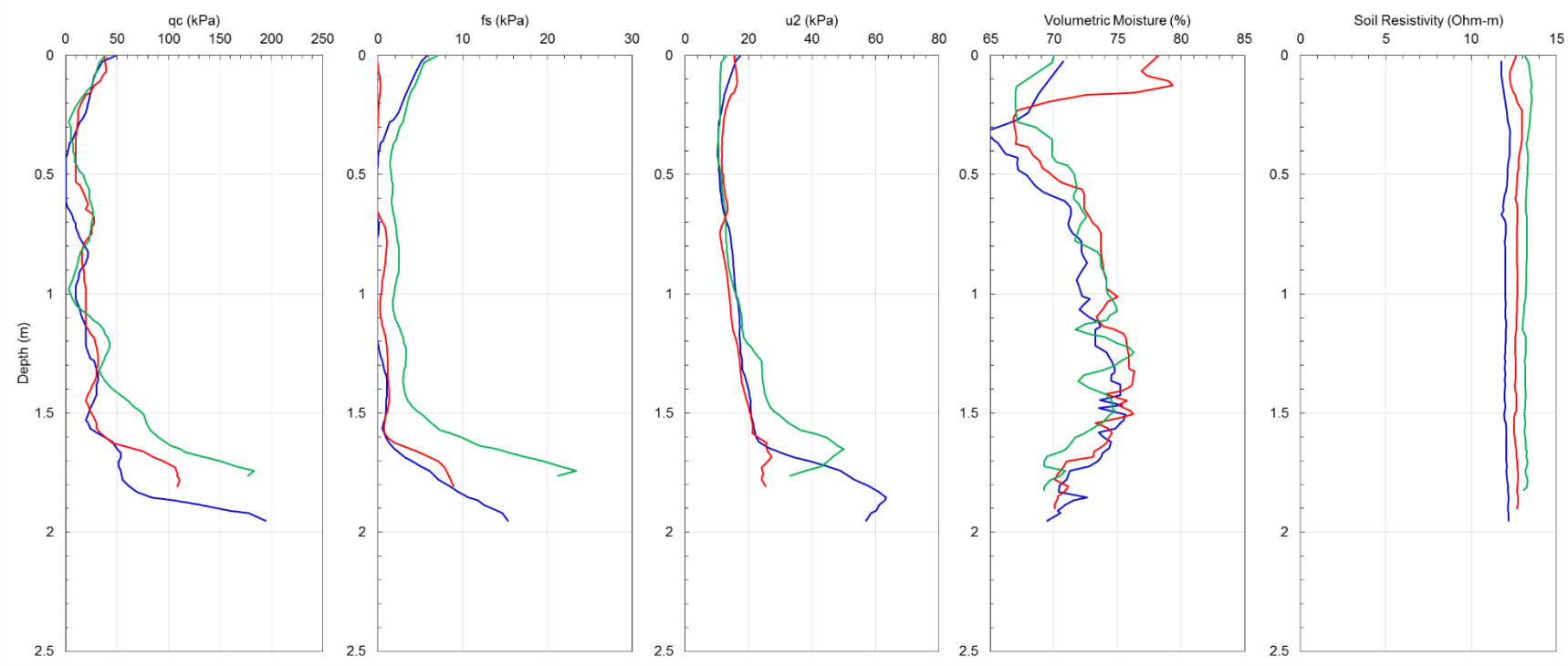

Fig. A21. CPTu soundings from Location 10, Site 1

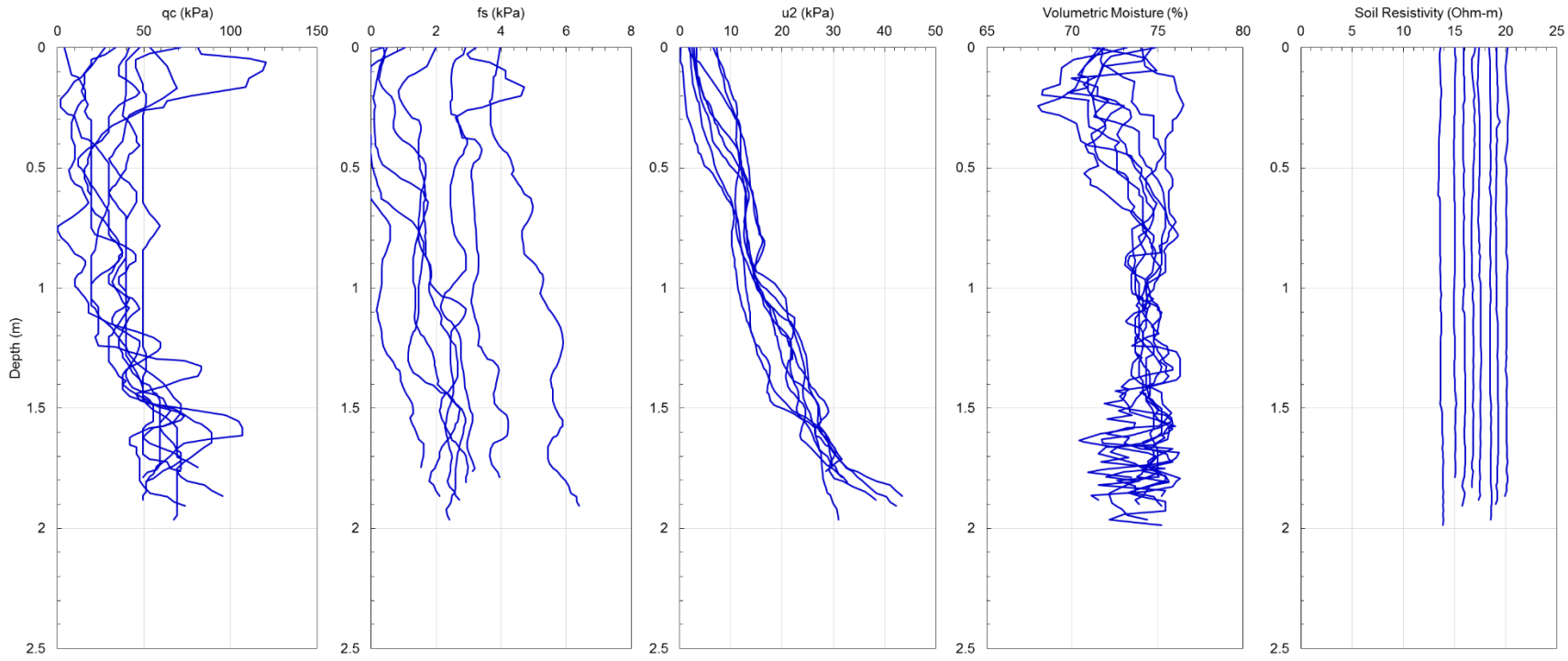

Fig. A22. CPTu soundings performed near the wave gauge installed by Parker (2014), Site 1